

Refined Study of Isocurvature Fluctuations in the Curvaton Scenario

Naoya Kitajima^{a,b}, David Langlois^c, Tomo Takahashi^d, and Shuichiro Yokoyama^{e,f}

^a*Department of Physics, Nagoya University, Nagoya 464-8602, Japan*

^b*Asia Pacific Center for Theoretical Physics, Pohang 37673, Korea*

^c*APC (Astroparticules et Cosmologie), CNRS-Université Paris Diderot, 10, rue Alice Domon
et Léonie Duquet, 75013 Paris, France*

^d*Department of Physics, Saga University, Saga 840-8502, Japan*

^e*Department of Physics, Rikkyo University, 3-34-1 Nishi-Ikebukuro, Toshima, Tokyo,
171-8501, Japan*

^f*Kavli IPMU (WPI), UTIAS, The University of Tokyo, Kashiwa, Chiba 277-8583, Japan*

Abstract

We revisit the generation of dark matter isocurvature perturbations in the curvaton model in greater detail, both analytically and numerically. As concrete examples, we investigate the cases of thermally decoupled dark matter and axionic dark matter. We show that the radiation produced by the decay of the curvaton, which has not been taken into account in previous analytical studies, can significantly affect the amplitude of isocurvature perturbations. In particular, we find that they are drastically suppressed even when the dark matter freeze-out (or the onset of the axion oscillations for axionic dark matter) occurs before the curvaton decays, provided the freeze-out takes place deep in the curvaton-dominated Universe. As a consequence, we show that the current observational isocurvature constraints on the curvaton parameters are not as severe as usually thought.

1 Introduction

Current cosmological data such as Planck [1, 2] have reached a high level of precision, thereby providing detailed information on the nature of primordial density fluctuations. Although the fluctuations of the inflaton are usually assumed to be directly at the origin of the observed density fluctuations, other possibilities can also be envisaged within the framework of inflation. For example, a scalar field other than the inflaton, whose energy density is negligible during inflation, could also generate primordial fluctuations, as in the curvaton scenario [3–5], which has been widely discussed in the literature. The current severe upper bound on the tensor-to-scalar r ratio^{#1} is compatible with this type of multi-field models, where r tends to be small.

In multi-field models, isocurvature fluctuations can also be produced in addition to the curvature perturbation. Although current observations have severely constrained the amplitude of isocurvature fluctuations [2], a small contribution is still allowed. Since isocurvature fluctuations can be associated with dark matter (DM) or baryons, a nonzero isocurvature perturbation would give precious information concerning models of DM or baryogenesis. In the curvaton model, the size of isocurvature fluctuations depends on when and how dark matter particles were created and/or the baryon asymmetry of the Universe was generated [7–12]. Therefore, even if isocurvature fluctuations are not observed, stringent upper bounds are also very useful to constrain models of DM and baryogenesis as they imply some restrictions on the generation mechanism of primordial fluctuations. In light of these considerations and given the current severe constraints, it is worth revisiting the issue of isocurvature fluctuations in the curvaton scenario in greater detail.

As a concrete example, we consider weakly interacting massive particles (WIMP) in curvaton models. In most previous studies, it has been considered that the size of isocurvature fluctuations is too large, given the present observational bounds, in models where WIMP dark matter freezes out *before* the curvaton decay, thus excluding such models. In the present work, we reexamine this standard lore by investigating the generation of isocurvature fluctuations in detail and show that, even if the freeze-out occurs before the curvaton decay, isocurvature fluctuations are significantly suppressed provided WIMPs freeze out deep in the curvaton-dominated era. In the curvaton scenario, the current upper limits on non-Gaussianity indicate that the curvaton should dominate the Universe at the time of its decay, which allows a DM freeze-out deep in the curvaton-dominated epoch. Hence our findings suggest that the non-detection of isocurvature fluctuations may not be as restrictive for curvaton models as previously thought.

In this article, we also investigate axionic DM in the curvaton scenario. In this case, the beginning of the axion oscillations is considered to be the critical time that determines the size of isocurvature fluctuations and it has been argued that, when the axion starts to oscillate before the curvaton decay, large (correlated) isocurvature fluctuations^{#2} are generated. However,

^{#1} From the combination of BICEP2/Keck Array, Planck and other data, the constraint on r is given as $r < 0.07$ (95 % C.L.) [6].

^{#2} Here, we have neglected the uncorrelated isocurvature perturbations of axion DM, which could be generated

similarly to the WIMP case, we show that, even when the onset of axion oscillations takes place before the curvaton decay, isocurvature fluctuations are drastically suppressed if it occurs deep in the curvaton-dominated epoch.

The organization of this paper is as follows. In the next section, we derive a general formula for super-Hubble density perturbations in a cosmological scenario where some transition (decay, freeze-out, ...) occurs in the early Universe. In this analytical derivation, we employ the usual approximation that the transition occurs instantaneously. In section 3, based on the derived formula we discuss DM isocurvature perturbations in the curvaton scenario for thermally decoupled DM such as WIMP. We also use of a numerical analysis and check the validity of the sudden transition approximation. As another example, we consider axionic DM, taking into account the temperature dependence for the axion mass. In section 4, we discuss the implications of our analysis for the isocurvature constraints on model parameters both in the WIMP and axion cases. The final section is devoted to the summary of our results.

2 Sudden transition formalism

Before investigating the DM isocurvature perturbations in the curvaton model, we present in this section a general formalism that enables us to determine analytically the density perturbations in a cosmological scenario where some transition (decay, freeze-out, ...) occurs in the early Universe. At the time of the transition, we consider only super-Hubble perturbations, which will later reenter the Hubble radius, and resort to the δN formalism [13–16]. In order to analytically follow the evolution of the perturbations during the transition, we adopt the so-called sudden transition approximation where the transition is supposed to occur instantaneously.

2.1 General formula

Even if the curvaton is a scalar field, it can be treated as a fluid once it starts to oscillate at the bottom of its potential. The corresponding equation of state depends on the shape of the potential. For example, an oscillating scalar field in a quadratic potential behaves as pressureless matter (i.e., its equation of state is $w = 0$), which we will assume from now on. Considering that all matter components are described as fluids, we can define for each individual fluid the nonlinear perturbation

$$\zeta_i = \delta N + \frac{1}{3(1+w_i)} \ln \left(\frac{\rho_i(t, \vec{x})}{\bar{\rho}_i(t)} \right), \quad (1)$$

where δN denotes the local perturbation of the number of e -folds, $\rho_i(t, \vec{x})$ is the energy density of the i -th component and $\bar{\rho}_i(t)$ its background homogeneous value; $w_i = \bar{P}_i/\bar{\rho}_i$ is the equation of state from the quantum fluctuations of the axion field.

of state parameter for the i -th fluid, \bar{P}_i being the background pressure. The definition of ζ_i in Eq. (1) can be inverted to give

$$\rho_i(t, \vec{x}) = \bar{\rho}_i e^{3(1+w_i)(\zeta_i - \delta N)}. \quad (2)$$

We now wish to study the evolution of the matter perturbations through a cosmological transition, which we assume to be instantaneous on the transition hypersurface \mathcal{H} defined by

$$H_{\mathcal{H}} = \Gamma_{\mathcal{H}}, \quad (3)$$

where H is the Hubble parameter and Γ is a physical quantity that depends on the nature of the transition: for a transition due to some particle decay, Γ corresponds to the decay rate; for a freeze-out transition, Γ represents the interaction rate.

By combining Eq. (3) and the (first) Friedmann equation, we can relate the (perturbed) energy density and the transition rate as

$$\frac{\rho_{\text{tot}}(t_{\mathcal{H}}, \vec{x})}{\bar{\rho}_{\text{tot}}(t_{\mathcal{H}})} = \frac{H^2(t_{\mathcal{H}}, \vec{x})}{\bar{H}^2(t_{\mathcal{H}})} = \frac{\Gamma^2(t_{\mathcal{H}}, \vec{x})}{\bar{\Gamma}^2(t_{\mathcal{H}})}, \quad (4)$$

where a bar denotes a background homogeneous quantity. Inserting in Eq. (4) the expression of the total energy density in terms of the individual ones,

$$\rho_{\text{tot}}(t_{\mathcal{H}}, \vec{x}) = \sum_i \rho_i(t_{\mathcal{H}}, \vec{x}) = \sum_i \bar{\rho}_i(t_{\mathcal{H}}) e^{3(1+w_i)(\zeta_i - \delta N_{\mathcal{H}})}, \quad (5)$$

we obtain

$$\sum_i \Omega_i(t_{\mathcal{H}}) e^{3(1+w_i)(\zeta_i - \delta N_{\mathcal{H}})} = \frac{\Gamma^2(t_{\mathcal{H}}, \vec{x})}{\bar{\Gamma}^2(t_{\mathcal{H}})}, \quad (6)$$

where we have introduced the background parameters $\Omega_i = \bar{\rho}_i(t)/(3M_{\text{pl}}^2 H^2)$.

In the following, we will restrict our analysis to linear perturbations, although we stress that the above formalism can easily be extended to nonlinear perturbations (see e.g. [17, 18]). Expanding Eq. (6) at linear order, we find that the transition hypersurface is characterized by the e -folding number perturbation

$$\delta N_{\mathcal{H}} = -\frac{2}{3\tilde{\Omega}} \delta_{\Gamma} + \frac{1}{\tilde{\Omega}} \sum_i \tilde{\Omega}_i \zeta_i, \quad (7)$$

where we have introduced the relative perturbation of the transition rate

$$\delta_{\Gamma} \equiv \frac{\Gamma(t_{\mathcal{H}}, \vec{x})}{\bar{\Gamma}(t_{\mathcal{H}})} - 1, \quad (8)$$

and the new background parameters

$$\tilde{\Omega}_i = (1 + w_i)\Omega_i, \quad \tilde{\Omega} = \sum_i \tilde{\Omega}_i = 1 + w_{\text{tot}}. \quad (9)$$

In the following, we consider a few particular cases which will be relevant for our study of isocurvature fluctuations generated in the curvaton model.

2.2 Case with $\Gamma = \text{constant}$

In the standard curvaton scenario, Γ is supposed to be constant. We can then easily recover the well-known results for the final density perturbation by setting $\delta_\Gamma = 0$ in Eq. (7). Before the curvaton decay, we have to take into account two fluids: the radiation originating from the inflaton and the oscillating curvaton, which we treat as non-relativistic matter. We thus find

$$\delta N_{\mathcal{H}} = \frac{3\Omega_\sigma \zeta_\sigma + 4\Omega_r \zeta_r}{3\Omega_\sigma + 4\Omega_r}, \quad (10)$$

where Ω_i and ζ_i are evaluated just before the decay. Since the total curvature perturbation ζ after the curvaton decay is given by $\zeta = \delta N_{\mathcal{H}}$, one obtains

$$\zeta = \frac{3\Omega_\sigma \zeta_\sigma + 4\Omega_r \zeta_r}{3\Omega_\sigma + 4\Omega_r}. \quad (11)$$

In the original curvaton scenario, the perturbation of inflaton-generated radiation ζ_r is neglected, so that

$$\zeta = r_{\text{dec}} \zeta_\sigma, \quad (12)$$

where r_{dec} is defined as

$$r_{\text{dec}} = \left. \frac{3\Omega_\sigma}{3\Omega_\sigma + 4\Omega_r} \right|_{\text{dec}}. \quad (13)$$

The more general formula (11) applies to the mixed curvaton and inflaton scenarios [19–24].

In order to compare the above analytic formula with numerical calculations, it is convenient to replace r_{dec} with the quantity [25]:

$$r_s \equiv \frac{3\rho_{r\sigma,f}}{3\rho_{r\sigma,f} + 4\rho_{r\phi,f}}, \quad (14)$$

where $\rho_{r\sigma,f}$ and $\rho_{r\phi,f}$ are the energy densities of radiations generated by the curvaton and the inflaton, respectively, evaluated well after the curvaton decay (with the ‘ f ’ subscript for “final”). Indeed, when one numerically follows the evolution of radiation and of the curvaton, one cannot define precisely the time of the curvaton decay. Some possible choices for the time of the curvaton decay are when $H = \Gamma$, or $\Gamma t = 1$ where t is the cosmic time, but these two choices, which give different values for r_{dec} , are somewhat arbitrary. By contrast, r_s defined in Eq. (14) does not depend on the decay time and thus avoids any ambiguity.

For later convenience, we also note that r_s is related to the amount of entropy produced during the curvaton decay, which can be expressed by the ratio

$$Q_s = \frac{\mathcal{S}_f}{\mathcal{S}_i}, \quad (15)$$

where \mathcal{S}_f and \mathcal{S}_i are entropies in a comoving volume respectively before and after the curvaton decay. Indeed, r_s can be written as

$$r_s = \frac{3(Q_s^{4/3} - 1)}{3Q_s^{4/3} + 1}. \quad (16)$$

2.3 Case with $\Gamma = \Gamma(T)$

When we consider the freeze-out of DM particles such as WIMPs, the reaction rate is given by $\Gamma = \langle \sigma_{\text{int}} v \rangle n_{\text{CDM}}$ where σ_{int} is the interaction cross section, v the relative velocity and n_{CDM} the WIMP number density. In this case, Γ depends on the temperature. For axionic dark matter, the transition occurs when the axion field starts to oscillate, i.e. when the Hubble parameter drops below the axion mass, m , which in principle depends on the temperature. In this case, we have $\Gamma = m(T)$.

Let us first derive a general expression that applies when Γ depends on the temperature, before discussing separately the particular cases of thermally decoupled DM and of axionic DM. Assuming that $\Gamma = \Gamma(T)$, one can write the fluctuations of Γ as

$$\delta_\Gamma = \alpha \delta_T, \quad (17)$$

where

$$\delta_T = \frac{\delta T}{T}, \quad \alpha = \frac{d \ln \Gamma}{d \ln T}. \quad (18)$$

Note that the above parameter α , whose explicit expression is model dependent, has also been adopted in [9]. Since the temperature is related to the radiation energy density as

$$T \equiv \left[\frac{30}{\pi^2 g_*} \rho_r \right]^{1/4}, \quad (19)$$

where g_* is the effective degrees of freedom, the temperature can be written as

$$T(t, \vec{x}) = \bar{T}(t) e^{\zeta_r - \delta N}, \quad (20)$$

which implies

$$\delta_T = \zeta_r - \delta N. \quad (21)$$

Inserting the relation (17) and (20) into Eq. (7), we arrive at

$$\delta N_{\mathcal{H}} = \frac{1}{3\tilde{\Omega} - 2\alpha} \left(3 \sum_i \tilde{\Omega}_i \zeta_i - 2\alpha \zeta_r \right). \quad (22)$$

Let us now discuss the fluctuations of DM. Regardless of whether DM particles are relativistic or non-relativistic, their number is conserved after the DM transition such as the freeze-out and the number density of DM particles n_c satisfies the following equation of motion in each homogeneous patch:

$$\frac{dn_c}{dt} + 3Hn_c = 0. \quad (23)$$

This implies that the local DM particle number density can be written as

$$n_c(t, \vec{x}) = \bar{n}_c(t) e^{3(\zeta_c - \delta N)}, \quad (24)$$

where ζ_c expresses the perturbation associated with the number density. Since in general n_c depends on the temperature only, one can relate the fluctuation of n_c to those of the temperature as

$$\frac{\delta n_c}{\bar{n}_c} = \frac{\partial \ln \bar{n}_c}{\partial \ln \bar{T}} \delta T = \nu \delta T, \quad (25)$$

where we have introduced the parameter

$$\nu \equiv \frac{\partial \ln \bar{n}_c}{\partial \ln \bar{T}}. \quad (26)$$

By evaluating the number density fluctuation on the transition hypersurface, expanding Eq. (24) at linear order, and substituting Eqs. (21) and (25), we finally obtain

$$\zeta_c = \frac{1}{3} [\nu \zeta_r + (3 - \nu) \delta N_{\mathcal{H}}]. \quad (27)$$

Assuming that only CDM and radiation are present after the transition, the CDM isocurvature perturbation S_c is usually defined by

$$S_c \equiv 3(\zeta_c - \zeta), \quad (28)$$

where ζ is the curvature perturbation for radiation, which coincides here with the adiabatic perturbation. In the curvaton model, ζ is given by Eq. (12). By deriving the expression ζ_c for some particular scenario of CDM generation, one can then predict the corresponding isocurvature fluctuations. As mentioned in the introduction, the isocurvature fluctuations are now severely constrained by the CMB observations and the amplitude of isocurvature perturbation can thus provide a crucial test for a variety of models. In the next section, we discuss thermally decoupled DM and axionic DM, both in the context of the curvaton model.

3 CDM Isocurvature fluctuations in the curvaton scenario

3.1 Thermally decoupled CDM

In this subsection, we study isocurvature fluctuations associated with thermally decoupled CDM in the curvaton model. As discussed in many papers (see e.g., [7–12]), a large CDM isocurvature perturbation is generated if CDM is created (or, equivalently, if its number density freezes out) *before* the curvaton decay, whereas no CDM isocurvature perturbation is generated when CDM is created *after* the curvaton decay. Here we revisit this issue in detail by using, on the one

hand, the sudden transition formalism developed in the previous section and, on the other hand, the numerical computation to follow the evolution of the homogeneous system^{#3}.

The equations of motion we need to solve are:

$$H^2 = \frac{1}{3M_{\text{pl}}^2} (\rho_r + \rho_\sigma + \rho_{\text{CDM}}) \simeq \frac{1}{3M_{\text{pl}}^2} (\rho_r + \rho_\sigma), \quad (29)$$

$$\frac{d\rho_r}{dt} + 4H\rho_r = \Gamma\rho_\sigma, \quad (30)$$

$$\frac{d\rho_\sigma}{dt} + 3H\rho_\sigma = -\Gamma\rho_\sigma, \quad (31)$$

$$\frac{dn_{\text{CDM}}}{dt} + 3Hn_{\text{CDM}} = -\lambda \left(n_{\text{CDM}}^2 - \left(n_{\text{CDM}}^{(\text{eq})} \right)^2 \right), \quad (32)$$

where ρ_r , ρ_σ and ρ_{CDM} are respectively the radiation, curvaton and CDM energy densities, and Γ is the decay rate of the curvaton. The first equation above is the Friedmann equation, where ρ_{CDM} can be neglected since we are in the very early Universe. The second and third equations describe, respectively, the evolution of the radiation and curvaton energy densities, where we assume that the curvaton behaves as non-relativistic matter. Their right-hand side characterizes the energy transfer between the curvaton and radiation as the curvaton decays.

The last equation, Eq. (32), describes the evolution of the CDM particle number density n_{CDM} , where, on the right hand side, λ denotes the thermally-averaged annihilation cross section of CDM particles: $\lambda = \langle \sigma_{\text{ann}} v \rangle$ with σ_{ann} and v being the cross section and relative velocity, respectively. The annihilation cross section can depend on the temperature as $\langle \sigma_{\text{ann}} v \rangle \propto T^q$ where the cases with $q = 0$ and 2 correspond to s -wave and p -wave annihilations, respectively. The right hand side also depends on the number density at equilibrium, $n_{\text{CDM}}^{(\text{eq})}$, which is given, for non-relativistic particles, by

$$n_{\text{CDM}}^{(\text{eq})} = g_{\text{CDM}} \left(\frac{mT}{2\pi} \right)^{3/2} e^{-m/T}, \quad (33)$$

where m is the mass of a CDM particle and g_{CDM} is the number of internal degrees of freedom.

3.1.1 Instantaneous transition formalism

When we consider thermally decoupled DM such as WIMPs, the freeze-out phase when DM particles decouple from the thermal bath corresponds to the transition after which the number of CDM particles is conserved. We define the instantaneous transition hypersurface by the relation

$$H = \Gamma = \langle \sigma_{\text{ann}} v \rangle n_{\text{CDM}}, \quad (34)$$

^{#3} The perturbations observed today were on super-Hubble scales at the time of the curvaton decay in the early Universe. For super-Hubble perturbations, it is sufficient to follow the homogeneous evolution of the various densities with slightly different initial conditions and compare them later in order to deduce the amplitude of the perturbations, in the spirit of the δN formalism.

where the number density at freeze-out can be approximated by the equilibrium expression (33). Taking into account the possible temperature dependence of the annihilation cross section, $\langle\sigma_{\text{ann}}v\rangle \propto T^{q/2}$, the parameter α defined in (18) is thus given by

$$\alpha = \frac{m}{T} + \frac{3}{2} + \frac{q}{2}. \quad (35)$$

Note that $m/T \sim 20$ at freeze out in the standard WIMP case. The parameter ν defined in Eq. (26) is given by

$$\nu = \frac{m}{T} + \frac{3}{2}. \quad (36)$$

Using this relation and the expression for $\delta N_{\mathcal{H}}$ in Eq. (7), one obtains

$$\zeta_c = \frac{1}{3} \left[\left(\frac{m}{T} + \frac{3}{2} \right) \zeta_r + \frac{1}{3\tilde{\Omega} - 2\alpha} \left(\frac{3}{2} - \frac{m}{T} \right) \left(3 \sum_i \tilde{\Omega}_i \zeta_i - 2\alpha \zeta_r \right) \right] \Big|_{\text{fr}}, \quad (37)$$

where all quantities on the right hand side are evaluated at the time of freeze-out, as indicated by the subscript ‘fr’.

In the scenarios where only radiation and the curvaton are present, the above expression reduces to

$$\zeta_c = \frac{1}{3} \left[\left(\frac{m}{T} + \frac{3}{2} \right) \zeta_r + \frac{1}{4 - 2\alpha - \Omega_\sigma} \left(\frac{3}{2} - \frac{m}{T} \right) \{ 3\Omega_\sigma \zeta_\sigma + (4 - 4\Omega_\sigma - 2\alpha) \zeta_r \} \right] \Big|_{\text{fr}}. \quad (38)$$

In the simplest curvaton models, one ignores the fluctuations of radiation produced by the inflaton. Substituting $\zeta_r = 0$ in (38), one thus gets

$$S_c/\zeta = 3 \left[\frac{\Omega_{\sigma,\text{fr}}}{r_{\text{dec}}} \left(\frac{3}{2} - \frac{m}{T_{\text{fr}}} \right) \frac{1}{4 - 2\alpha_{\text{fr}} - \Omega_{\sigma,\text{fr}}} - 1 \right], \quad (39)$$

where the subscript ‘fr’ means that the corresponding quantity is evaluated at the time of freeze-out. This equation has already been derived in [9].

Eq. (39) works rather well when the radiation produced by the curvaton decay is negligible at the time of freeze-out. However, in comparison with the radiation produced by the inflaton decay, the radiation generated by the curvaton decay can become significant. When the freeze-out occurs after the curvaton dominates the Universe, the latter type of radiation constitutes most of the radiation component. In this case, neglecting the radiation perturbation is not valid anymore since the perturbation of the curvaton-generated radiation is similar to the initial curvaton perturbation. We discuss this point in more detail in the numerical study that follows. In Appendix A, we also present a modified version of our formalism where we artificially separate the two types of radiation and treat them as distinct components ($\rho_r = \rho_{r\phi} + \rho_{r\sigma}$ where ρ_r is the total radiation energy density and $\rho_{r\phi}$ and $\rho_{r\sigma}$ are respectively the inflaton- and curvaton-generated radiation), which can give some insight about how the CDM perturbation and the isocurvature fluctuations evolve.

Before moving to the numerical study, let us briefly mention two limiting cases, which have already been discussed in the literature:

- **Case where the freeze-out occurs after the curvaton decay**

In this case, by putting $\Omega_\sigma = 0$ in Eq. (38), we obtain $\zeta_c = \zeta_r$. Therefore, when the freeze-out occurs after the curvaton decay, one finds

$$S_c = 0. \quad (40)$$

No isocurvature fluctuations are generated in this case.

- **Case where the freeze-out occurs during RD epoch (the curvaton never dominates the Universe before the freeze-out)**

When the freeze-out occurs during RD epoch and the curvaton never dominates the Universe before the freeze-out, we can put $\Omega_\sigma = 0$. In addition, since radiation is essentially the product of the inflaton decay in this case, we can assume $\zeta_r = 0$ (neglecting the inflaton fluctuations) and Eq. (38) yields $\zeta_c = 0$. Therefore, we obtain

$$\frac{S_c}{\zeta} = -3, \quad (41)$$

which is completely excluded by current observations.

3.1.2 Numerical evolution

We now investigate the isocurvature fluctuations more precisely by resorting to a numerical calculation based on the δN formalism. In this calculation, we numerically solve the background equations along two trajectories with different initial values for the curvaton energy density. After solving the background equations, we evaluate the difference of the energy density of each component (radiation and DM) at a final time when the curvaton has completely decayed into radiation. This final time is defined on a hypersurface with a uniform e -folding number (see Eq. (1)).

The background evolution of the energy densities ρ_σ (red solid), $\rho_{r\phi}$ (orange dotted), and $\rho_{r\sigma}$ (blue dashed), in terms of the number of e -folds, is plotted in the upper panels of Fig. 1 for two cases: in the left panel ($Q_s = 1.1$), the curvaton always remains subdominant, whereas in the right panel ($Q_s = 1000$) it dominates the energy budget before its decay.

In the lower panels of Fig. 1, we plot the residual CDM isocurvature perturbation, or more precisely the quantity $-S_c/\zeta$, as a function of the number of e -folds between the CDM freeze-out and the curvaton decay, i.e. $N_{\text{dec}} - N_{\text{fr}}$ (where the curvaton decay time is defined by $t_{\text{dec}} = \Gamma^{-1}$ and the freeze-out time by $H = \lambda n_{\text{CDM}}^{(\text{eq})}$). The red points correspond to the fully numerical results, while the blue points are obtained with the analytical prediction from Eq. (38). The blue points should be regarded as resulting from a semi-analytic calculation,

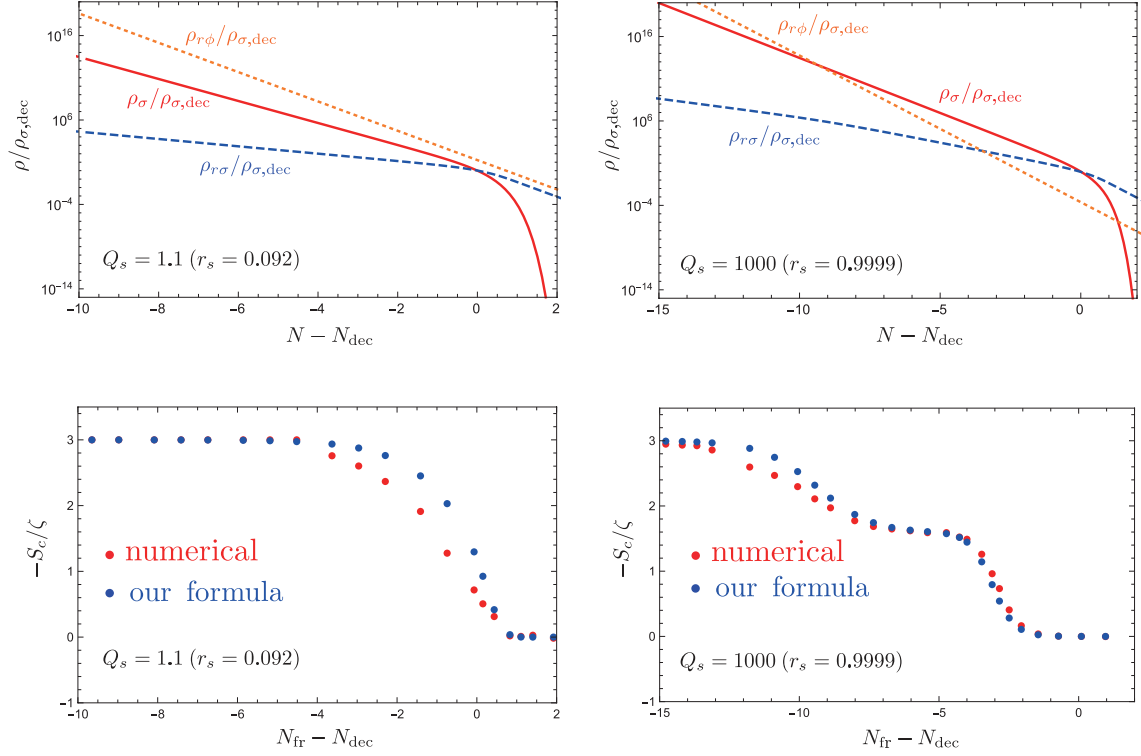


Figure 1: The upper panels show the evolution of background energy density of the curvaton ρ_{σ} (red solid), the inflaton-generated radiation $\rho_{r\phi}$ (orange dotted), and the curvaton-generated radiation $\rho_{r\sigma}$ (blue dashed), as a function of e -folding number measured from the decay time of the curvaton ($N = N_{\text{dec}}$). In this plot, N_{dec} corresponds to the time $t_{\text{dec}} = \Gamma^{-1}$. The lower panels show the residual CDM isocurvature perturbations as a function of the time of CDM freeze out ($N = N_{\text{fr}}$) measured from N_{dec} . The red points in these panels are numerical results and the blue points are the ones calculated semi-analytically from Eq. (38). Left panels are for the case with $Q_s = 1.1$ and right panels are for the case with $Q_s = 1000$. In this calculation, we fix λ and the freeze-out temperature is changed by varying m . The temperature dependence of the annihilation cross section is fixed to be $q = 0$.

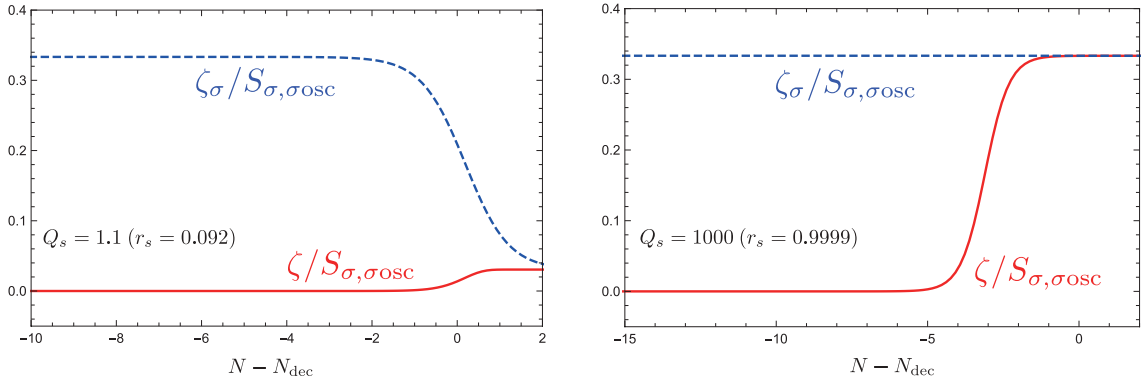


Figure 2: The evolution of ζ (red line) and ζ_σ (blue dashed line) for $Q_s = 1.1$ (left panel) and $Q_s = 1000$ (right panel), as functions of $N - N_{\text{dec}}$. Here the vertical axis is normalized by $S_{\sigma, \sigma \text{osc}}$ which is the isocurvature perturbation of the curvaton ($S_\sigma := 3(\zeta_\sigma - \zeta)$) at the time of the onset of the curvaton oscillations (defined by $m_\sigma = H(N_{\sigma \text{osc}})$).

since we use the formula (38) with the values of $\zeta_r(N_{\text{fr}})$ and $\zeta_\sigma(N_{\text{fr}})$ at freeze-out time, obtained from the numerical evolution of ζ_r (red line) and ζ_σ (blue dashed line) as shown in Fig. 2.

The lower panels of Fig. 1 show that our formula is mostly consistent with the numerical result in both cases. One can clearly see the two limiting behaviours already discussed, $S_c/\zeta \simeq -3$ and $S_c/\zeta \simeq 0$ when the freeze-out takes place, respectively, long before or long after the curvaton decay. In the case $Q_s = 1.1$, these two limits are separated by a transition of roughly 5 e -folds. By contrast, in the case with $Q_s = 1000$, where the curvaton reaches domination before its decay, one can see that there exists an intermediate region where $-S_c/\zeta \approx 1.5$. Moreover, one notes that $-S_c/\zeta$ is strongly suppressed even for negative values of $N_{\text{fr}} - N_{\text{dec}}$, i.e. even when the freeze-out occurs before the completion of the curvaton decay.

By comparing the behavior of the residual CDM isocurvature perturbations with the background dynamics shown in the upper panel, we can see that the range of $N_{\text{fr}} - N_{\text{dec}}$ where $-S_c/\zeta \approx 1.5$ corresponds to a phase when the curvaton dominates the Universe while the radiation component is dominated by the inflaton-generated component. If the freeze-out occurs during such an era, one can substitute $\zeta_r = 0$ and $\Omega_{\sigma, \text{fr}} \approx r_s \approx 1$ in the expression (38), which implies [9]

$$-S_c/\zeta \approx -3 \left[\left(\frac{3}{2} - \frac{m}{T_{\text{fr}}} \right) \frac{1}{3 - 2\alpha_{\text{fr}}} - 1 \right]. \quad (42)$$

Assuming $m/T_{\text{fr}} \gg 1$, and hence $\alpha_{\text{fr}} \approx m/T_{\text{fr}}$ according to (35), yields $S_c/\zeta \approx -3/2$.

Next let us focus on the region where S_c/ζ goes to zero when the freeze-out occurs (slightly) before the curvaton decay. This region corresponds to the era where the matter-like curvaton dominates the Universe while the radiation component is also dominated by the curvaton-generated one. In this regime, the Universe is completely dominated by the two components

associated with the curvaton and, in this sense, evolves adiabatically. Therefore, the residual CDM isocurvature perturbations also vanish in this limit.

Once the value of Q_s is given, we can estimate the duration of the period during which the radiation component is completely dominated by the curvaton-generated radiation, before the curvaton decay. This duration can be represented by the quantity $N_{\text{dec}} - N_{\text{dom}}$ as a function of Q_s , where N_{dom} is defined as the time when the curvaton-generated radiation starts to dominate the inflaton-generated radiation (i.e., $\rho_{r\sigma}(N_{\text{dom}}) = \rho_{r\phi}(N_{\text{dom}})$)^{#4} When Q_s is large, it can be approximated as

$$Q_s \simeq \left(\frac{\rho_{r\sigma}}{\rho_{r\phi}} \right)^{3/4}, \quad (43)$$

where the right-hand side is evaluated at the time of the curvaton decay. Since $\rho_{r\sigma}$ and $\rho_{r\phi}$ respectively scale as $\rho_{r\sigma} \propto a^{-3/2}$ (for the curvaton-dominated Universe) and $\rho_{r\phi} \propto a^{-4}$, and using the definition of N_{dom} , one can derive

$$N_{\text{dom}} - N_{\text{dec}} \simeq \frac{8}{15} \ln Q_s, \quad (44)$$

which gives the time when the isocurvature fluctuations vanish once Q_s is given.

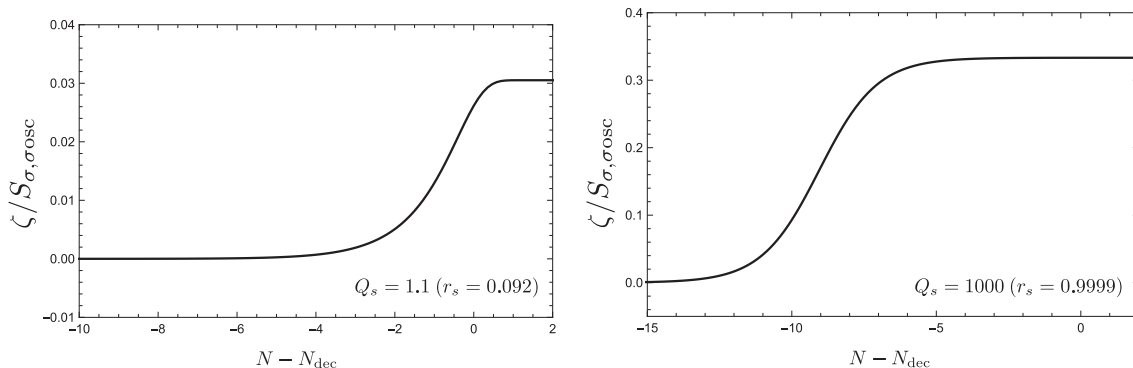


Figure 3: The evolution of ζ as a function of $N - N_{\text{dec}}$ for $Q_s = 1.1$ (left panel) and $Q_s = 1000$ (right panel). As in Fig. 2, the vertical axis is normalized by $S_{\sigma,\sigma\text{osc}}$.

3.1.3 Difference between the analytical and numerical results

Let us briefly discuss the deviation between our analytic formula and the numerical result shown in Fig. 1. The sudden transition formalism (38) uses the value of each curvature perturbation at freeze-out but does not depend on the information about how the perturbations evolve. In order to show that the time variation of ζ could be relevant to explain the deviation between

^{#4} In the following, the subscript ‘dom’ indicates that the quantity is evaluated at time of $N = N_{\text{dom}}$.

the analytical and numerical results, we plot the evolution of the curvature perturbation ζ , as a function of the number of e -folds $N - N_{\text{dec}}$ in Fig. 3. Comparing this figure with Fig. 1, one notices that ζ starts to evolve significantly in the regions where the deviation between the numerical result and the sudden transition formalism becomes large as shown in Fig. 1. Nevertheless we should stress that the basic behavior of the CDM isocurvature perturbations can be understood by the use of the sudden transition formalism (38).

3.2 Axion DM

The role of DM can also be played by an oscillating scalar field, such as an axion [26–29] (see also e.g. [30, 31] for recent reviews on cosmological aspects of axion DM). Denoting the axion field as χ and assuming that its potential is of the form $V(\chi) = m^2\chi^2/2$ (at least at the bottom of the potential), its equation of motion is given by

$$\ddot{\chi} + 3H\dot{\chi} + m^2(T)\chi = 0, \quad (45)$$

where $m(T)$ is the axion mass and can depend on the temperature above a critical temperature T_{cr} :

$$m(T) \simeq \begin{cases} m_*(T_{\text{cr}}/T)^\beta & \text{for } T > T_{\text{cr}} \\ m_* & \text{for } T < T_{\text{cr}} \end{cases}. \quad (46)$$

For the ordinary QCD axion, one has $\beta = 3.34$, $T_{\text{cr}} = 0.26\Lambda_{\text{QCD}}$ with $\Lambda_{\text{QCD}} = 400$ MeV and $m_* = 3.82 \times 10^{-2} \Lambda_{\text{QCD}}^2 / F_a \simeq 6 \times 10^{-6} \text{ eV} (10^{12} \text{ GeV} / F_a)$, F_a being the axion decay constant [32].

The production of axions occurs via the so-called misalignment mechanism. The initial amplitude of the axion oscillations is given by $\chi_i = F_a\theta_i$, where θ_i is an initial misalignment angle. Just after the axion field begins to oscillate, the axion number density is given by

$$n_\chi = \frac{1}{2m(T)}(\dot{\chi}^2 + m^2(T)\chi^2), \quad (47)$$

and then evolves adiabatically as $n_\chi \propto a^{-3}$.

One can consider that axion DM is “created” at the sudden transition hypersurface that corresponds to the onset of the axion oscillations, defined by

$$H(N_{\chi\text{osc}}) = m(N_{\chi\text{osc}}), \quad (48)$$

where $N_{\chi\text{osc}}$ denotes the number of e -folds at the onset of the axion oscillations. From the above temperature-dependence of the axion mass, given in Eq. (46), we can easily calculate the coefficients α and ν , introduced in Eqs. (18) and (26) respectively, and we get

$$\alpha = \nu = -\beta. \quad (49)$$

Substituting these relations into Eqs. (22) and (27), the DM perturbation is found to be given by

$$\zeta_c = \frac{1}{3} \left[-\beta\zeta_r + \frac{3+\beta}{3\tilde{\Omega} + 2\beta} \left(3 \sum_i \tilde{\Omega}_i \zeta_i + 2\beta\zeta_r \right) \right] \Big|_{\chi\text{osc}}, \quad (50)$$

where the quantities on the right hand side are evaluated at the onset of the axion oscillations.

In the context of the curvaton scenario, where only radiation and the curvaton fluid are present, the above formula reduces to

$$\zeta_c = \frac{1}{3} \left[-\beta\zeta_r + \frac{3 + \beta}{4 + 2\beta - \tilde{\Omega}_\sigma} \{3\Omega_\sigma\zeta_\sigma + (4 - 4\Omega_\sigma + 2\beta)\zeta_r\} \right] \Big|_{\chi_{\text{osc}}}. \quad (51)$$

By putting $\zeta_r = 0$, which is assumed in the original curvaton model, one can write the isocurvature fluctuation for the axion DM as

$$S_c/\zeta = 3 \left(\frac{\Omega_{\sigma,\chi_{\text{osc}}}}{r_{\text{dec}}} \frac{3 + \beta}{4 + 2\beta - \Omega_{\sigma,\chi_{\text{osc}}}} - 1 \right). \quad (52)$$

This formula has also been obtained in [9]. However, as we already stressed in the WIMP case, the assumption of $\zeta_r = 0$ is not really justified when radiation is dominated by its curvaton generated component at the onset of the axion oscillations.

Fig. 4 shows the comparison between our numerical results (red points) and the semi-analytic formula (50) using the values of ζ_r and ζ_σ obtained numerically, with the following choice of parameters: $\beta = 3.34$, $F_a = 10^{12}$ GeV and $m_\sigma = 10^6$ GeV with $Q_s = 1.1$ (left), and 1000 (right). While the numerical result presents an overall good agreement with our analytic formula, there is nevertheless some difference between them. In particular, a bump appears near $\Delta N \equiv N_{\chi_{\text{osc}}} - N_{\text{dec}} \simeq 4$ in the case of $Q_s = 1000$ (right panel of Fig. 4). This is due to the fact that DM is an oscillating scalar field. In the sudden transition approximation, we assume that the axion comoving number density is instantaneously fixed at the beginning of the axion oscillations and then conserved. However, this conservation is strictly valid only for an adiabatic evolution, which takes place later when $m \gg H$. In practice, this condition is not yet fully satisfied just after the onset of oscillations. Thus, the final value is sensitive to the change of the oscillation frequency (or time derivative of the axion mass, \dot{m}) at that time. It becomes maximal when the equation of state for the radiation component changes significantly due to the curvaton generated radiation. Fig. 5 shows the difference between the realistic case (the numerical result in Fig. 4(b)) and an idealized case where the axion number density is initially determined by the expression (47), at the time when $H = m(T)$, and then assumed to evolve as $n_\chi \propto a^{-3}$. The latter case clearly satisfies the adiabatic condition and, as a consequence, the bump does not appear.

4 Implications for the constraints on model parameters

We now discuss the implications of our results concerning the constraints on the model parameters in the curvaton scenario. So far, it has been argued in the literature that, when the transition that produces DM occurs before the curvaton decay, sizable isocurvature fluctuations are generated, which is inconsistent with observations. However, as shown in the previous section, isocurvature fluctuations can be suppressed even when the freeze-out occurs before the

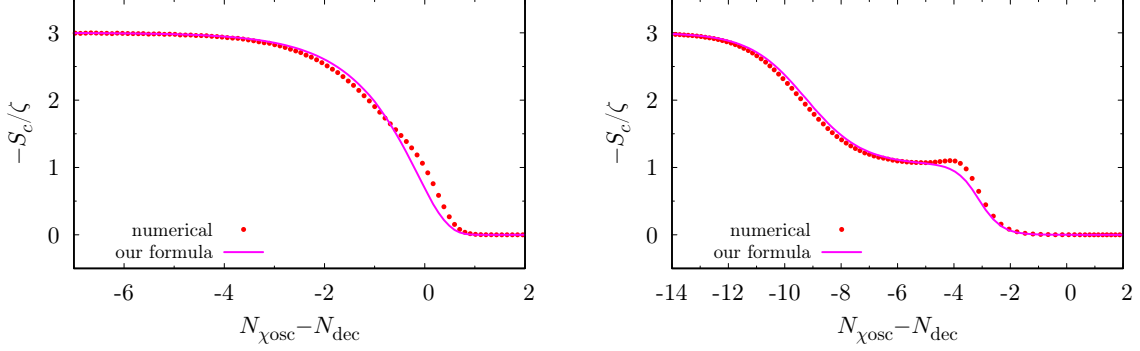


Figure 4: Plot of $-S_c/\zeta$ as a function of $N_{\chi\text{osc}} - N_{\text{dec}}$ for the cases with $\beta = 3.34$ and $F_a = 10^{12}$ GeV and $m_\sigma = 10^6$ GeV. The magenta line represents the semi-analytic formula (50). We show the cases with $Q_s = 1.1$ (left), and 1000 (right). Here $N_{\chi\text{osc}}$ and N_{dec} are the e -folding numbers at $H = m(T)$ and $\Gamma t = 1$ respectively.

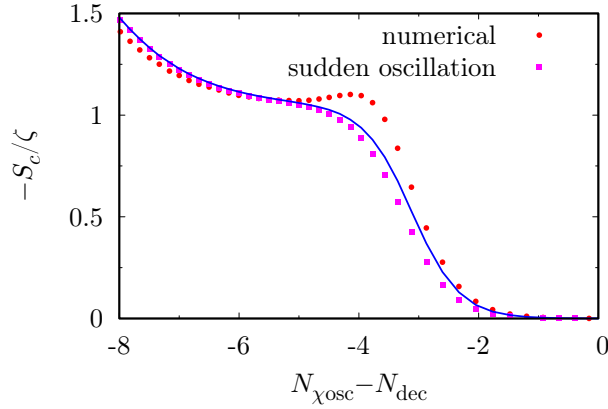


Figure 5: Comparison between the numerical result in Fig. 4(b) (red circles) and the “sudden oscillation” case where the axion number density is set to evolve as $n_\chi \propto a^{-3}$ just after the epoch of $H = m(T)$ (magenta squares).

curvaton decay provided the radiation generated by the curvaton decay is the main component in the radiation.

In this section, we discuss the constraints on the initial amplitude of the curvaton σ_* and its decay rate Γ that can be deduced from the non-detection of isocurvature fluctuations. Indeed, the isocurvature fluctuations are severely constrained by the present CMB observations, such as those of Planck. Isocurvature and adiabatic perturbations produced in multi-field inflationary scenarios can be correlated, as shown in [33], and the CMB constraints depend on the degree of correlation between the isocurvature and the adiabatic perturbations. In the curvaton scenario considered here, isocurvature perturbations are negatively correlated with adiabatic ones^{#5}. As a conservative estimate, we adopt here the isocurvature upper bound

$$\left| \frac{S_c}{\zeta} \right| < 0.1, \quad (53)$$

from which we derive constraints on σ_* and Γ . In the following, we present our results for the WIMP and axion cases, successively.

Before discussing the isocurvature constraints, it should be noted that these parameters can also be constrained by non-Gaussianity^{#6}. Indeed, Planck observations have tightly constrained the so-called non-linearity parameter f_{NL} . In the curvaton scenario, the non-Gaussianity is of the local type and the corresponding limits are given by $f_{\text{NL}}^{(\text{local})} = 2.5 \pm 5.7$ (68 % C.L.) [38], from which one derives a lower bound on r_{dec} :

$$r_{\text{dec}} > 0.16 \quad (68 \text{ \% C.L.}). \quad (54)$$

Since this quantity can be approximated by [4]

$$r_{\text{dec}} \sim \text{Min} \left[1, \left(\frac{\sigma_*}{M_{\text{pl}}} \right)^2 \left(\frac{m_\sigma}{\Gamma} \right)^{1/2} \right], \quad (55)$$

where σ_* is the initial amplitude of the curvaton, we get that the allowed region in the σ_* - Γ is characterized by

$$\frac{\Gamma}{M_{\text{pl}}} \lesssim 10^{-13} \left(\frac{m_\sigma}{10^6 \text{ GeV}} \right) \left(\frac{\sigma_*}{M_{\text{pl}}} \right)^4. \quad (56)$$

We will take into account the constraint from non-Gaussianity when we show our results on the isocurvature constraints.

^{#5} Generally in the curvaton scenario, where DM is produced from the curvaton decay, the so-called positively correlated isocurvature fluctuations are generated. By contrast, when DM is not produced directly from the curvaton decay but from another sector, one gets negatively correlated isocurvature perturbations, as the scenarios discussed in this paper.

^{#6} We consider here the non-Gaussianity of the dominant adiabatic mode. Note that the isocurvature modes also lead to non-Gaussianities, which differ from the adiabatic ones, although they are usually subdominant except in special models [17, 34–37].

4.1 WIMP case

We start with the case of WIMP dark matter. In Fig. 6, we show the region excluded by the isocurvature constraint, together with the one from non-Gaussianity (green region) given by Eq. (54). Here, we have taken $m_{\text{WIMP}} = 1$ TeV, $m_\sigma = 10^6$ GeV, and have tuned the thermally-averaged annihilation cross section of WIMP, λ , so that $\Omega_{\text{WIMP}} h^2 = 0.12$ [1].

When the curvaton dominates the total energy density before its decay, the final abundance of DM is modified from the one calculated in the standard scenario. Here we derive an approximate expression for the theoretically-expected Ω_{WIMP} in such a case. Freeze-out is characterized by

$$H_{\text{fr}} = \lambda n_{\text{WIMP,fr}}^{(\text{eq})}, \quad (57)$$

and

$$H_{\text{fr}}^2 = \frac{\rho_{r,\text{fr}}}{3M_{\text{pl}}^2} (1 - \Omega_{\sigma,\text{fr}})^{-1}. \quad (58)$$

Taking account of the entropy production from the curvaton, in the case where the freeze-out occurs before the curvaton decay, that is, $T_{\text{fr}} > T_{\text{dec}}$, the density parameter of WIMP at the present time can be evaluated as

$$\Omega_{\text{WIMP}} h^2 = \frac{m_{\text{WIMP}} n_{\text{WIMP},0}}{\rho_{\text{crit}}/h^2} = m_{\text{WIMP}} \frac{n_{\text{WIMP},0}}{s_0} \frac{s_0}{\rho_{\text{crit}}/h^2} = m_{\text{WIMP}} R_s^{-1} \frac{n_{\text{WIMP,fr}}}{s(T_{\text{fr}})} \frac{s_0}{\rho_{\text{crit}}/h^2}, \quad (59)$$

where ρ_{crit} is the critical energy density and s_0 is the entropy density at the present time. R_s is the dilution factor given by the ratio of the entropy at the freeze-out time and that after the curvaton decay,

$$R_s := \frac{\mathcal{S}_f}{\mathcal{S}_{\text{fr}}} = Q_s \frac{\mathcal{S}_i}{\mathcal{S}_{\text{fr}}}, \quad (60)$$

where Q_s is defined in Eq. (15) and can be expressed as

$$Q_s = \frac{\mathcal{S}_f}{\mathcal{S}_i} = \max \left[1, \left. \frac{4}{3T_{\text{dec}}} \frac{\rho_\sigma}{s} \right|_{\text{osc}} \right] = \max \left[1, \frac{1}{6} \left(\frac{m_\sigma}{\Gamma_\sigma} \right)^{1/2} \left(\frac{\sigma_*}{M_{\text{pl}}} \right)^2 \right], \quad (61)$$

where we have used

$$\left. \frac{4}{3T_{\text{dec}}} \frac{\rho_\sigma}{s} \right|_{\text{osc}} = \frac{T_{\text{osc}}}{T_{\text{dec}}} \Omega_{\sigma,\text{osc}} = \frac{1}{6} \frac{T_{\text{osc}}}{T_{\text{dec}}} \left(\frac{\sigma_*}{M_{\text{pl}}} \right)^2 = \frac{1}{6} \left(\frac{m_\sigma}{\Gamma_\sigma} \right)^{1/2} \left(\frac{\sigma_*}{M_{\text{pl}}} \right)^2. \quad (62)$$

By assuming the instantaneous decay of the curvaton at $t = t_{\text{dec}}$, that is, neglecting the contribution of the curvaton-generated radiation before the curvaton decay ($t = t_{\text{dec}}$), we have $\mathcal{S}_i = \mathcal{S}_{\text{fr}}$ for the case with $T_{\text{fr}} > T_{\text{dec}}$, which implies $R_s = Q_s$. However, once the curvaton-generated radiation is taken into account, $\mathcal{S}_i/\mathcal{S}_{\text{fr}}$ should depend on when the WIMP freeze-out

occurs even before the curvaton decay. By using $\rho_{\text{crit}}/s_0 h^2 = 3.64 \times 10^{-9}$ GeV and assuming that $g_{*,\text{fr}} = g_{*,\text{fr}} = 106.75$, we get

$$\Omega_{\text{WIMP}} h^2 \simeq 0.12 \left(\frac{m_{\text{WIMP}}/T_{\text{fr}}}{20} \right) \left(\frac{3.3 \times 10^9 \text{ GeV}^{-1}}{\lambda M_{\text{pl}}} \right) \times \begin{cases} 1 & \text{for } T_{\text{fr}} < T_{\text{dec}} \\ (1 - \Omega_{\sigma,\text{fr}})^{-1/2} R_s^{-1} & \text{for } T_{\text{fr}} > T_{\text{dec}} \end{cases}. \quad (63)$$

Here, we have used $n_{\text{WIMP},\text{fr}} = n_{\text{WIMP},\text{fr}}^{(\text{eq})} = H_{\text{fr}}/\lambda$ based on Eqs. (57) and (58). The expression for $T_{\text{fr}} > T_{\text{dec}}$ can be further divided into 3 cases, which we now discuss in turn.

• **Case 1 : freeze-out occurs during inflaton-generated radiation dominated era**

When the WIMP freeze-out occurs during the inflaton-generated radiation domination before the curvaton decay, we can take $\Omega_{\sigma,\text{fr}} \rightarrow 0$ and $R_s = Q_s$ in Eq. (63). Then, Ω_{WIMP} is simply given as

$$\Omega_{\text{WIMP}} h^2 \simeq 0.12 \left(\frac{m_{\text{WIMP}}/T_{\text{fr}}}{20} \right) \left(\frac{3.3 \times 10^9 \text{ GeV}^{-1}}{\lambda M_{\text{pl}}} \right) Q_s^{-1}. \quad (64)$$

• **Case 2 : freeze-out occurs during curvaton dominated era with $T_{\text{fr}} > T_{\text{dom}}$**

In the case where the freeze-out occurs during the curvaton domination, we should take into account the factor $(1 - \Omega_{\sigma,\text{fr}})$. Since here the freeze-out occurs before the curvaton-generated radiation becomes dominant in the total radiation component, i.e., $T_{\text{fr}} > T_{\text{dom}}$, the factor R_s should still be identical to Q_s , and hence we have in this case

$$\Omega_{\text{WIMP}} h^2 \simeq 0.12 \left(\frac{m_{\text{WIMP}}/T_{\text{fr}}}{20} \right) \left(\frac{3.3 \times 10^9 \text{ GeV}^{-1}}{\lambda M_{\text{pl}}} \right) (1 - \Omega_{\sigma,\text{fr}})^{-1/2} Q_s^{-1}, \quad (65)$$

where $(1 - \Omega_{\sigma,\text{fr}})$ is given by

$$\begin{aligned} 1 - \Omega_{\sigma,\text{fr}} &= \frac{\rho_{r,\text{fr}}}{3M_{\text{pl}}^2 H_{\text{fr}}^2} \simeq \frac{\rho_{r,\text{fr}}}{\rho_{\sigma,\text{fr}}} = \frac{\rho_{r,\text{osc}}}{\rho_{\sigma,\text{osc}}} \left(\frac{T_{\text{fr}}}{T_{\text{osc}}} \right) \\ &= 6 \left(\frac{90}{\pi^2 g_{*,\text{osc}}} \right)^{-1/4} \left(\frac{\sigma_*}{M_{\text{pl}}} \right)^{-2} \left(\frac{m_\sigma}{M_{\text{pl}}} \right)^{-1/2} \left(\frac{m_{\text{WIMP}}}{M_{\text{pl}}} \right) \left(\frac{T_{\text{fr}}}{m_{\text{WIMP}}} \right). \end{aligned} \quad (66)$$

• **Case 3 : freeze-out occurs during curvaton dominated era with $T_{\text{fr}} < T_{\text{dom}}$**

When the freeze-out occurs after the domination of the curvaton-generated radiation over the inflaton-generated radiation (but note that the total energy density of the Universe is still dominated by the curvaton), the factor $(1 - \Omega_{\sigma,\text{fr}})$ becomes different from Eq. (66) and can be expressed as

$$1 - \Omega_{\sigma,\text{fr}} = \frac{\rho_{r\sigma,\text{fr}}}{3M_{\text{pl}}^2 H_{\text{fr}}^2} = \frac{\rho_{r\sigma,\text{fr}}}{\rho_{r\sigma,\text{fr}} + \rho_{\sigma,\text{fr}}} \simeq \frac{(T_{\text{dec}}/T_{\text{fr}})^4}{1 + (T_{\text{dec}}/T_{\text{fr}})^4}, \quad (67)$$

where we have used $\rho_{r\sigma,\text{dec}} \simeq \rho_{\sigma,\text{dec}}$, and the scaling $\rho_r \simeq \rho_{r\sigma} \propto a^{-3/2}$ for $T_{\text{dom}} > T_{\text{fr}} > T_{\text{dec}}$. Moreover, we have

$$\frac{T_{\text{dec}}}{T_{\text{fr}}} \simeq \left(\frac{90}{\pi^2 g_{*,\text{dec}}} \right)^{1/4} \left(\frac{m_{\text{WIMP}}}{T_{\text{fr}}} \right) \left(\frac{m_{\text{WIMP}}}{M_{\text{pl}}} \right)^{-1} \left(\frac{\Gamma}{M_{\text{pl}}} \right)^{1/2}. \quad (68)$$

Furthermore, the factor R_s is not identical to the total entropy production ratio Q_s because $\mathcal{S}_i/\mathcal{S}_{\text{fr}} \neq 1$ due to the contribution of the curvaton-generated radiation. By using the scaling for the energy density of the curvaton-generated radiation given by $\rho_{r\sigma} \propto a^{-3/2}$ [40], we find

$$\frac{\mathcal{S}_i}{\mathcal{S}_{\text{fr}}} = \frac{T_i^3 a_i^3}{T_{\text{fr}}^3 a_{\text{fr}}^3} = \frac{T_{\text{dom}}^3 a_{\text{dom}}^3}{T_{\text{fr}}^3 a_{\text{fr}}^3} = \left(\frac{a_{\text{dom}}}{a_{\text{fr}}} \right)^{-9/8} \left(\frac{a_{\text{dom}}}{a_{\text{fr}}} \right)^3 = e^{-\frac{15}{8}(N_{\text{fr}} - N_{\text{dom}})}, \quad (69)$$

from which we get the relation

$$R_s = e^{-\frac{15}{8}(N_{\text{fr}} - N_{\text{dom}})} Q_s. \quad (70)$$

In conclusion, we have for this case

$$\Omega_{\text{WIMP}} h^2 \simeq 0.12 \left(\frac{m_{\text{WIMP}}/T_{\text{fr}}}{20} \right) \left(\frac{3.3 \times 10^9 \text{ GeV}^{-1}}{\lambda M_{\text{pl}}} \right) (1 - \Omega_{\sigma,\text{fr}})^{-1/2} Q_s^{-1} e^{\frac{15}{8}(N_{\text{fr}} - N_{\text{dom}})}. \quad (71)$$

The extra factor $e^{\frac{15}{8}(N_{\text{fr}} - N_{\text{dom}})}$ can also be expressed in terms of the model parameters as

$$\begin{aligned} e^{\frac{15}{8}(N_{\text{fr}} - N_{\text{dom}})} &= \left(\frac{a_{\text{fr}}}{a_{\text{dom}}} \right)^{15/8} = \left(\frac{T_{\text{fr}}}{T_{\text{dom}}} \right)^{-5} \\ &\simeq 8 \times 10^{-3} \left(\frac{T_{\text{fr}}}{m_{\text{WIMP}}} \right)^{-5} \left(\frac{m_{\text{WIMP}}}{M_{\text{pl}}} \right)^{-5} \left(\frac{\Gamma}{M_{\text{pl}}} \right)^2 \left(\frac{m_{\sigma}}{M_{\text{pl}}} \right)^{1/2} \left(\frac{\sigma_*}{M_{\text{pl}}} \right)^2. \end{aligned} \quad (72)$$

(This can be obtained by using the expression for T_{dom} which is given later in Eq. (83) in Section 4.1.2.)

We expect the above expressions for $\Omega_{\text{WIMP}} h^2$ to give only a rough estimate of the final DM abundance, within one order of magnitude. We have also computed the precise prediction of Ω_{WIMP} by resorting to a numerical computation, defining the ‘‘correction’’ factor A as $\Omega_{\text{WIMP}}|_{\text{numerical}} = A^{-1} \Omega_{\text{WIMP}}|_{\text{analytical}}$. In the case where $Q_s \gg 1$ and $N_{\text{dec}} > N_{\text{fr}} > N_{\text{dom}}$, we have found that a correction factor $A \simeq 2.5$ is required. We have also found that $A \simeq 1.8$ for the case where $Q_s \gg 1$ and $N_{\text{fr}} < N_{\text{dom}}$ and $A \simeq 1.1$ for $Q_s \simeq 1$.

In Ref. [39], a more precise analytic formula for Ω_{WIMP} has been proposed by using a different definition of the freeze-out time. We have extended this method to apply it to cases for which late time entropy production is significant and obtained an analytic formula for Ω_{WIMP} which is in better agreement with the numerical results. In particular, in the case where $Q_s \gg 1$ and

$N_{\text{dec}} > N_{\text{fr}} > N_{\text{dom}}$, the correction factor is reduced to $A \simeq 1.7$. The derivation of this analytic formula is given in Appendix B.

In Fig. 6, the blue dashed line corresponds to the isocurvature constraint obtained by naively requiring that the freeze-out occurs before the curvaton decay, i.e., $N_{\text{fr}} > N_{\text{dec}}$, as usually assumed in former works. To determine the region where $N_{\text{fr}} > N_{\text{dec}}$ is satisfied, we have numerically calculated the background evolutions of ρ_r and ρ_σ . By contrast, the red region corresponds to the constraint derived by numerically evaluating S_c , which automatically includes the effects of the curvaton-generated radiation. For both traditional and revised constraints, we resort to numerical calculation, even if some rough analytic estimates can be derived, as we discuss below.

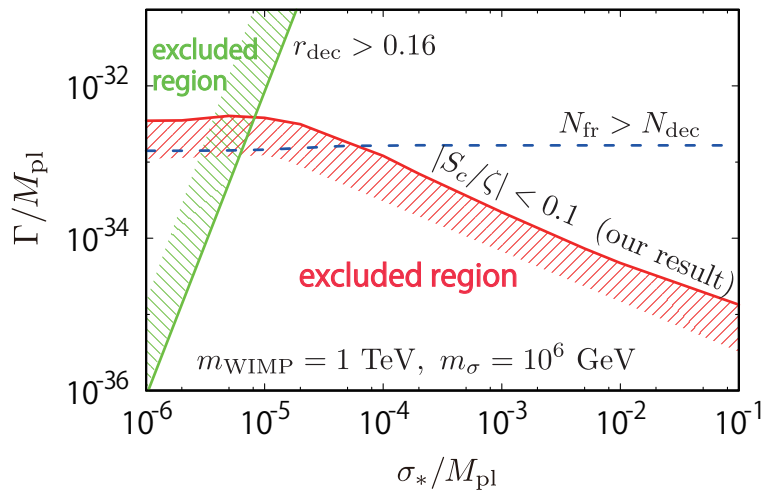


Figure 6: Excluded region from the isocurvature constraints along the one from non-Gaussianity (green region) in the σ_* - Γ space. The red region is our result and the blue one corresponds to the conventional constraint $N_{\text{fr}} > N_{\text{dec}}$. Here, we have chosen the illustrative values $m_{\text{WIMP}} = 1 \text{ TeV}$, $m_\sigma = 10^6 \text{ GeV}$, and have tuned the thermally-averaged annihilation cross section of WIMP so that $\Omega_{\text{WIMP}} h^2 = 0.12$. The allowed region is top right one.

4.1.1 Conventional constraint

We have evaluated N_{fr} and N_{dec} by numerically solving the evolution of the system but it is also instructive to understand the constraint via an analytic estimate. The constraint derived from $N_{\text{dec}} < N_{\text{fr}}$ can be expressed as

$$\frac{T_{\text{fr}}}{T_{\text{dec}}} < 1. \quad (73)$$

In order to realize $\Omega_{\text{WIMP}} h^2 = 0.12$ the freeze out temperature is such that $m_{\text{WIMP}}/T_{\text{fr}} \simeq 20$ (with our choice $m_{\text{WIMP}} = 1$ TeV). On the other hand, T_{dec} is determined by Γ as

$$\frac{g_* \pi^2}{30} T_{\text{dec}}^4 = M_{\text{pl}}^2 \Gamma^2, \quad (74)$$

where the decay time is defined by $\Gamma = H$. Therefore the requirement of Eq. (73) leads to

$$\frac{m_{\text{WIMP}}}{20} \lesssim \left(\frac{30}{g_* \pi^2} \right)^{1/4} M_{\text{pl}}^{1/2} \Gamma^{1/2}, \quad (75)$$

from which we obtain

$$\frac{\Gamma}{M_{\text{pl}}} \gtrsim 10^{-33} \left(\frac{m_{\text{WIMP}}}{1 \text{ TeV}} \right)^2. \quad (76)$$

As expected, no σ_* dependence appears in the constraint. Going back to Fig. 6, we can see that the above formula provides a good estimate for the conventional constraint indicated by the blue dashed line.

4.1.2 New constraint

In Fig. 6, the red excluded region is obtained by requiring $|S_c/\zeta| > 0.1$ where S_c/ζ is calculated numerically and the effects of the curvaton-generated radiation are automatically included as mentioned above. In comparison with the previous region satisfying $N_{\text{fr}} > N_{\text{dec}}$ (blue dashed line), the new allowed region is significantly larger, as a consequence of taking the curvaton-generated radiation effect into account, particularly when the curvaton dominates the Universe early and the curvaton-generated radiation then becomes the main component of radiation.

To understand better this new constraint, an analytical argument is helpful. As shown in the previous section, when the curvaton-generated radiation becomes dominant in the radiation component, the isocurvature fluctuations are significantly suppressed and the constraint $|S_c/\zeta| < 0.1$ can be easily satisfied. Therefore the allowed parameter region can be roughly estimated by

$$N_{\text{dom}} < N_{\text{fr}}. \quad (77)$$

Instead of Eq. (77), we can also use the following equivalent relation to derive the constraint:

$$\frac{T_{\text{fr}}}{T_{\text{dom}}} < 1. \quad (78)$$

When the curvaton-generated radiation is the main component in radiation, the Universe is dominated by the curvaton. In such case, the energy density of the curvaton-generated radiation scales as $\rho_{r\sigma} \propto a^{-3/2}$ [40], then the cosmic temperature is determined by

$$T^4 \propto \rho_{r\sigma} \propto a^{-3/2}. \quad (79)$$

Based on this relation, T_{dom} can be estimated as

$$T_{\text{dom}} = T_{\text{dec}} \left(\frac{a_{\text{dom}}}{a_{\text{dec}}} \right)^{-3/8} = \left(\frac{90}{g_{*,\text{dec}}\pi^2} \right)^{1/4} (\Gamma M_{\text{pl}})^{1/2} \left(\frac{a_{\text{dom}}}{a_{\text{dec}}} \right)^{-3/8}. \quad (80)$$

By using the fact that there is no entropy production between $N_{\sigma\text{osc}}$ and N_{dom} , we also get

$$T_{\text{dom}} = T_{\sigma\text{osc}} \left(\frac{a_{\text{dom}}}{a_{\sigma\text{osc}}} \right)^{-1} = \left(\frac{90}{g_{*,\sigma\text{osc}}\pi^2} \right)^{1/4} (m_{\sigma} M_{\text{pl}})^{1/2} \left(\frac{a_{\text{dom}}}{a_{\sigma\text{osc}}} \right)^{-1}, \quad (81)$$

where $a_{\sigma\text{osc}}$ is the scale factor at the onset of the curvaton oscillations. In addition, provided the curvaton dominates the universe at the decay, $a_{\text{dec}}/a_{\sigma\text{osc}}$ can be derived as follows,

$$\frac{a_{\text{dec}}}{a_{\sigma\text{osc}}} = \left(\frac{\rho_{\sigma}(t_{\text{dec}})}{\rho_{\sigma}(t_{\sigma\text{osc}})} \right)^{-1/3} = \left(\frac{3\Gamma^2 M_{\text{pl}}^2}{\frac{1}{2}m_{\sigma}^2\sigma_*^2} \right)^{-1/3} = \frac{1}{6^{1/3}} \left(\frac{\Gamma}{m_{\sigma}} \right)^{-2/3} \left(\frac{\sigma_*}{M_{\text{pl}}} \right)^{2/3}. \quad (82)$$

From these equations, we obtain

$$\frac{T_{\text{dom}}}{m_{\text{WIMP}}} \simeq 0.38 \times \left(\frac{m_{\text{WIMP}}}{M_{\text{pl}}} \right)^{-1} \left(\frac{\Gamma}{M_{\text{pl}}} \right)^{2/5} \left(\frac{m_{\sigma}}{M_{\text{pl}}} \right)^{1/10} \left(\frac{\sigma_*}{M_{\text{pl}}} \right)^{2/5}. \quad (83)$$

By using the above equations, we find that the isocurvature constraint can be written as

$$\frac{\Gamma}{M_{\text{pl}}} \gtrsim 10^{-38} \times \left(\frac{m_{\text{WIMP}}/T_{\text{fr}}}{20} \right)^{-5/2} \left(\frac{m_{\text{WIMP}}}{1 \text{ TeV}} \right)^{5/2} \left(\frac{m_{\sigma}}{10^6 \text{ GeV}} \right)^{-1/4} \left(\frac{\sigma_*}{M_{\text{pl}}} \right)^{-1}. \quad (84)$$

In fact, the numerical result in Fig. 6 shows that the actual isocurvature constraint (red line) is slightly larger than the above analytic estimate. The difference can be explained as follows. As shown in Fig. 1 the isocurvature perturbations are actually suppressed not exactly for $N_{\text{fr}} - N_{\text{dom}} \gtrsim 0$ but rather for $N_{\text{fr}} - N_{\text{dom}} \gtrsim \gamma$ ($\gamma \simeq 2$). By taking into account this correction factor, γ , the constraint (78) can be rewritten as

$$\frac{T_{\text{dom}}}{T_{\text{fr}}} > e^{3\gamma/8}, \quad (85)$$

where we have used $T \propto a^{-3/8}$ for $N > N_{\text{dom}}$. As a consequence, the lower bound for Γ given in Eq. (84) is multiplied by a factor $e^{15\gamma/16}$.

Furthermore, for $\sigma_*/M_{\text{pl}} \gtrsim 10^{-2}$, the dependence of the lower bound for Γ on σ_*/M_{pl} seems to become weaker than $\propto (\sigma_*/M_{\text{pl}})^{-1}$ shown in Eq. (84). This feature can be qualitatively understood as follows. This region in parameter space corresponds to the case where the freeze-out occurs during when the curvaton-generated radiation dominates in the radiation component, and the constraint is basically expressed as $T_{\text{fr}} < T_{\text{dom}}$. In this case, the expression for Ω_{WIMP} is given by Eq. (71) and, with the help of Eq. (72), it can be written as

$$\Omega_{\text{WIMP}} h^2 \simeq 0.12 \left(\frac{m_{\text{WIMP}}/T_{\text{fr}}}{20} \right) \left(\frac{3.3 \times 10^9 \text{ GeV}^{-1}}{\lambda M_{\text{pl}}} \right)$$

$$\times (1 - \Omega_{\sigma, \text{fr}})^{-1/2} \left(\frac{m_{\text{WIMP}}/T_{\text{fr}}}{20} \right)^5 \left(\frac{m_{\text{WIMP}}}{1 \text{ TeV}} \right)^{-5} \left(\frac{\Gamma}{1.5 \times 10^{-33} M_{\text{pl}}} \right)^{5/2}. \quad (86)$$

Recall that larger σ_* and smaller Γ generate larger entropy production by the decay of the curvaton, that is, larger Q_s . A larger entropy production thus tends to reduce the relic abundance Ω_{WIMP} , as indicated by the dependence of Γ in Eq. (86). But, as already mentioned, in our calculation we fix the relic abundance at $\Omega_{\text{WIMP}} h^2 \simeq 0.12$, and hence for larger Q_s (corresponding to smaller Γ) we take λ smaller in order to keep Ω_{WIMP} unchanged, which makes the freeze-out epoch earlier (i.e., $m_{\text{WIMP}}/T_{\text{fr}}$ becomes smaller (roughly, $m_{\text{WIMP}}/T_{\text{fr}} \propto \ln \lambda$) and the right hand side in Eq. (84) becomes larger).

From the non-Gaussianity constraint, the parameter space where the curvaton dominates the Universe when it decays is preferred. Importantly, in such a region, the curvaton-generated radiation also tends to be dominant in the radiation component and the isocurvature fluctuations are significantly suppressed. This means that part of the parameter space which was believed to be excluded by the isocurvature constraints is in fact allowed.

4.2 Axion DM

4.2.1 Abundance

We now present our results for axionic DM, taking into account the entropy production due to the curvaton decay and the effects of the curvaton-generated radiation. The final abundance of the axion DM depends on the details of the scenario. One can distinguish three cases as listed below.

- **Case 1 : axion oscillations begin during RD era (before/after the curvaton decay)**

In the case where the axion starts to oscillate during radiation domination, either before or after the curvaton decay, one has^{#7}

$$H = m(T) \quad \text{with} \quad H = \left(\frac{\pi^2 g_*}{90} \right)^{1/2} \frac{T^2}{M_{\text{pl}}}, \quad (87)$$

which leads to

$$T_{\chi_{\text{osc}}} \simeq 1 \text{ GeV} \left(\frac{F_a}{10^{12} \text{ GeV}} \right)^{-\frac{1}{\beta+2}}. \quad (88)$$

Here and in what follows, we set $g_{*\chi_{\text{osc}}} = 80$ as an indicative reference value. The ratio between the axion number density and the entropy density at that time is

$$\left. \frac{n_\chi}{s} \right|_{\chi_{\text{osc}}} = \left. \frac{T}{8m(T)} \right|_{\chi_{\text{osc}}} \left(\frac{\chi_i}{M_{\text{pl}}} \right)^2. \quad (89)$$

^{#7} Conventionally, the beginning of the axion oscillation is defined by $3H = m(T)$ in the literature. In this paper, however, we adopt the same definition as Eq. (48) which is used to calculate the isocurvature perturbation. This affects the final abundance by a factor of about 2.

From now on, we set $\chi_i = F_a$ ($\theta_i = 1$) for simplicity. n_χ is an adiabatic invariant quantity but if the curvaton decay occurs after the axion production, it is diluted by the entropy production due to the curvaton decay. The resultant density parameter of the axion CDM is obtained by multiplying the entropy dilution factor, Q_s^{-1} , defined by Eq. (15), a correction factor κ associated with the non-adiabaticity and the present axion mass and being divided by $\rho_{\text{crit}}/s_0 h^2$

$$\Omega_\chi h^2 \simeq 0.02 \kappa \left(\frac{F_a}{10^{12} \text{ GeV}} \right)^{\frac{\beta+3}{\beta+2}} \times \begin{cases} 1 & \text{for } T_{\chi\text{osc}} < T_{\text{dec}} \\ Q_s^{-1} & \text{for } T_{\chi\text{osc}} > T_{\text{dec}} \end{cases}. \quad (90)$$

We have estimated the correction factor by taking the ratio between analytic and numerical results of the final axion abundance and found $\kappa \sim 5$ in this case. In the case where the axion starts to oscillate when the fraction of the energy density of the curvaton becomes large, κ can be as large as 8.

• **Case 2 : axion oscillation begins during σ D era and $T_{\chi\text{osc}} > T_{\text{dom}}$**

If the axion oscillations begin in the curvaton dominated era, but while the radiation component is still dominated by the inflaton-generated radiation, the Hubble parameter at the onset of axion oscillations is given by

$$H_{\chi\text{osc}} = \frac{\rho_\sigma^{1/2}(t_{\chi\text{osc}})}{\sqrt{3}M_{\text{pl}}} = \frac{\rho_\sigma^{1/2}(t_{\text{osc}})}{\sqrt{3}M_{\text{pl}}} \left(\frac{T_{\chi\text{osc}}}{T_{\text{osc}}} \right)^{3/2}, \quad (91)$$

and we obtain

$$T_{\chi\text{osc}} = 0.08 \text{ GeV} \left(\frac{m_\sigma}{10^6 \text{ GeV}} \right)^{-\frac{1}{4(\beta+3/2)}} \left(\frac{\sigma_*}{M_{\text{pl}}} \right)^{-\frac{1}{\beta+3/2}} \left(\frac{F_a}{10^{12} \text{ GeV}} \right)^{-\frac{1}{\beta+3/2}}. \quad (92)$$

The initial energy density of the axion is related to that of the curvaton through

$$\frac{\rho_\chi}{\rho_\sigma} \Big|_{\chi\text{osc}} = \frac{\frac{1}{2}m(T)^2 F_a^2}{3H^2 M_{\text{pl}}^2} \Big|_{\chi\text{osc}} = \frac{1}{6} \left(\frac{F_a}{M_{\text{pl}}} \right)^2, \quad (93)$$

and by using the conservation of ρ_σ/s , one obtains

$$\frac{\rho_\chi}{s} \Big|_{\chi\text{osc}} = \frac{\rho_\chi}{\rho_\sigma} \Big|_{\chi\text{osc}} \frac{\rho_\sigma}{s} \Big|_{\chi\text{osc}} = \frac{1}{6} \left(\frac{F_a}{M_{\text{pl}}} \right)^2 \frac{\rho_\sigma}{s} \Big|_{\text{osc}} \frac{\mathcal{S}_i}{\mathcal{S}_{\chi\text{osc}}} = \frac{1}{48} T_{\text{osc}} \left(\frac{\sigma_*}{M_{\text{pl}}} \right)^2 \left(\frac{F_a}{M_{\text{pl}}} \right)^2 \frac{\mathcal{S}_i}{\mathcal{S}_{\chi\text{osc}}}. \quad (94)$$

Because the curvaton dominates the Universe at the curvaton decay, a significant amount of entropy is produced. Hence the present value of ρ_χ/s can be given by

$$\frac{\rho_\chi}{s} \Big|_0 = \frac{\mathcal{S}_{\chi\text{osc}}}{\mathcal{S}_f} \frac{\kappa m_*}{m(T_{\chi\text{osc}})} \frac{\rho_\chi}{s} \Big|_{\chi\text{osc}} = \frac{\kappa T_{\text{dec}} m_*}{8m(T_{\chi\text{osc}})} \left(\frac{F_a}{M_{\text{pl}}} \right)^2, \quad (95)$$

where we have used Eq. (61) in the last equality. Finally, one can obtain the present density parameter of the axion DM,

$$\Omega_\chi h^2 = 3 \times 10^{-7} \kappa \left(\frac{m_\sigma}{10^6 \text{ GeV}} \right)^{-\frac{\beta}{4\beta+6}} \left(\frac{\sigma_*}{M_{\text{pl}}} \right)^{-\frac{\beta}{\beta+3/2}} \left(\frac{T_{\text{dec}}}{0.1 \text{ GeV}} \right) \left(\frac{F_a}{10^{12} \text{ GeV}} \right)^{\frac{\beta+3}{\beta+3/2}}. \quad (96)$$

By comparing with our numerical results, we have found $\kappa \sim 3.5$. However κ can be as large as 5 near the boundary between cases 1 and 2.

• **Case 3 : axion oscillations begin during σ D era and $T_{\chi\text{osc}} < T_{\text{dom}}$**

In this case, $T_{\chi\text{osc}}$ is determined by the temperature of the curvaton-generated radiation,

$$T = \left(\frac{10g_{*\text{dec}}}{\pi^2 g_*^2} \right)^{1/8} (3HT_{\text{dec}}^2 M_{\text{pl}})^{1/4}, \quad (97)$$

where H is to be replaced with $m(T)$. Then the temperature at the onset of axion oscillation is

$$T_{\chi\text{osc}} = 0.5 \text{ GeV} \left(\frac{T_{\text{dec}}}{0.1 \text{ GeV}} \right)^{\frac{2}{\beta+4}} \left(\frac{F_a}{10^{12} \text{ GeV}} \right)^{-\frac{1}{\beta+4}}, \quad (98)$$

where we set $g_{*\text{dec}} = 10$ and $g_{*\text{dom}} = 80$. Substituting it into Eq. (95), the density parameter of the axion CDM is found to be given by

$$\Omega_\chi h^2 = 1 \times 10^{-4} \kappa \left(\frac{T_{\text{dec}}}{0.1 \text{ GeV}} \right)^{\frac{3\beta+4}{\beta+4}} \left(\frac{F_a}{10^{12} \text{ GeV}} \right)^{\frac{\beta+8}{\beta+4}}, \quad (99)$$

where $\kappa \sim 1.5$ in this case.

4.2.2 Conventional constraint

According to the conventional argument, the axion should start to oscillate after the curvaton decay in order to be consistent with the present upper bound on isocurvature perturbations. This corresponds to the constraint $N_{\chi\text{osc}} > N_{\text{dec}}$ or $T_{\chi\text{osc}} < T_{\text{dec}}$. Because the universe is dominated by radiation after the curvaton decay, one can use Eq. (88) for $T_{\chi\text{osc}}$. Note that there is no entropy production after the onset of the axion oscillations and F_a can be fixed by using Eq. (90) if we assume $\Omega_\chi = \Omega_{\text{DM}}$. Then, $T_{\chi\text{osc}} < T_{\text{dec}}$ leads to

$$\frac{\Gamma}{M_{\text{pl}}} \gtrsim \frac{m_a(T_{\chi\text{osc}})}{M_{\text{pl}}} \simeq 10^{-36}, \quad (100)$$

thus providing an upper bound on the decay rate of the curvaton, which corresponds to the dashed blue horizontal line in Fig. 7.

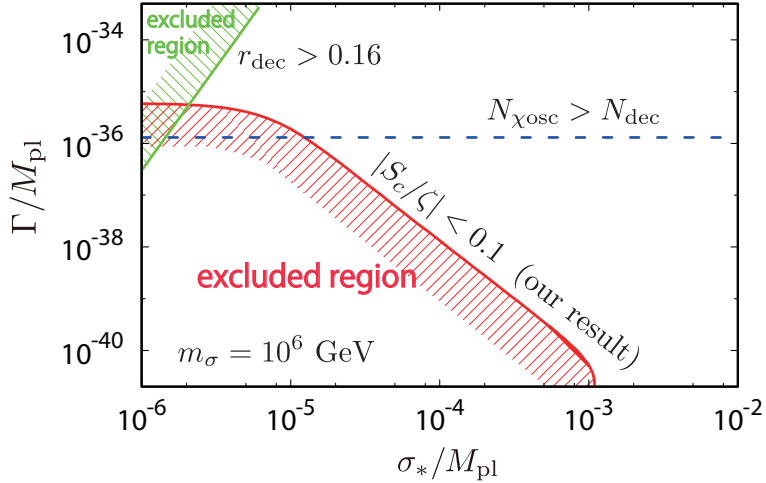


Figure 7: Isocurvature and non-Gaussianity constraints in the Γ - σ_* plane for axion DM, obtained numerically. The red curve is our new constraint and the blue horizontal line is the conventional constraint. The green line shows the constraint from f_{NL} . We have taken $m_\sigma = 10^6$ GeV and $\beta = 3.34$ (corresponding to the QCD axion case). The allowed region is the top right part of the figure.

4.2.3 New constraint

We have shown in the previous section that the isocurvature constraint is milder than previously thought and is roughly given by $T_{\text{dom}} \gtrsim T_{\chi\text{osc}}$. In this situation, one can use Eq. (98) for $T_{\chi\text{osc}}$. F_a can be fixed by using Eq. (99) with $\Omega_\chi = \Omega_{\text{DM}}$ and $T_{\text{dom}} \gtrsim T_{\chi\text{osc}}$ leads to

$$\frac{\Gamma}{M_{\text{pl}}} \gtrsim 1 \times 10^{-50} \times \kappa^{\frac{10}{4\beta+7}} \left(\frac{m_\sigma}{10^6 \text{ GeV}} \right)^{-\frac{\beta+8}{4\beta+7}} \left(\frac{\sigma_*}{M_{\text{pl}}} \right)^{-\frac{4(\beta+8)}{4\beta+7}}. \quad (101)$$

Fig. 7 shows numerical result of the excluded region in Γ - σ_* plane. The region below the red curve is excluded by the CDM isocurvature constraint $|S_c/\zeta| < 0.1$, which translates into the inequality (101). The dashed blue horizontal line corresponds to the conventional upper bound, discussed earlier, and the green line represents the constraint from non-Gaussianity. Similarly to the WIMP case, one can also take into account the correction factor $\gamma \equiv N_{\chi\text{osc}} - N_{\text{dom}}$, which entails a multiplication of the right hand side in Eq. (101) by $e^{\frac{15(\beta+8)}{4(4\beta+7)}\gamma}$. Comparing the analytic formula with the numerical result, we have found $\gamma \simeq 3$. Finally, one notes that the red line drops sharply near $\sigma_*/M_{\text{pl}} \sim 10^{-3}$. This is due to the disappearance of the temperature dependence of the axion mass (see Eq. (46)).

5 Conclusion

In this paper, we have made a detailed investigation of DM isocurvature fluctuations in the curvaton scenario, when DM is composed of WIMPs or axions, and revisited the constraints that can be inferred from the non-observation of isocurvature perturbations in the CMB. In previous works, it is usually considered that isocurvature fluctuations are too large to be consistent with observations as soon as DM is created before the curvaton decay.

However, in the present work, we have found that more scenarios are still acceptable. Indeed, one can still include models where DM is created before the completion of the curvaton decay, provided the DM freeze-out (for WIMPs, or the onset of oscillations for axions) occurs when the curvaton-generated radiation dominates the radiation component. In this situation, the isocurvature perturbations are also suppressed. Interestingly, curvaton scenarios where the curvaton tends to dominate the energy content of the Universe over a long period of time are favoured by the current constraints on primordial non-Gaussianity.

In summary, our results show that the usual constraints on curvaton models from isocurvature fluctuations can be partially relaxed, thus opening a new window for viable scenarios. In this paper, we have only investigated the isocurvature fluctuations associated with DM. Similar argument should also hold for baryonic isocurvature perturbations, which could lead to useful consequences for models of baryogenesis in the framework of the curvaton scenario. Furthermore, it would be interesting to study other type of CDM such as feebly interacting massive particle (FIMP) [41], strongly interacting massive particle (SIMP) [42, 43].

Acknowledgments

T.T would like to thank APC for its hospitality during his visit, where part of this work has been done. This work is partially supported by JSPS KAKENHI Nos. 15H05888 (TT, SY), 15K05084 (TT), 15K17659 (SY) and 16H01103 (SY). N.K. acknowledges the support by Grant-in-Aid for JSPS Fellows and the Max-Planck-Gesellschaft, the Korea Ministry of Education, Science and Technology, Gyeongsangbuk-Do and Pohang City for the support of the Independent Junior Research Group at the Asia Pacific Center for Theoretical Physics.

A Formalism with curvaton-generated radiation

As mentioned in Section 3.1.1, it has been usually considered that sizable isocurvature fluctuations are generated when WIMP DM particles freeze out before the curvaton decay, or a scalar field such as the axion begins to oscillate before the curvaton decay. However, if the curvaton-generated radiation dominates over that produced by the inflaton sector, the isocurvature

fluctuations are drastically suppressed. We have demonstrated this via numerical calculations as well as semi-analytic derivations in Section 3.1.1.

In this appendix, we show that the suppression of isocurvature fluctuations can also be recovered via a fully analytic derivation based on the (somewhat artificial) separation of the total radiation energy density ρ_r into two components,

$$\rho_r = \rho_{r\phi} + \rho_{r\sigma}, \quad (102)$$

where $\rho_{r\phi}$ and $\rho_{r\sigma}$ are the energy densities of the radiations produced by the inflaton and by the curvaton, respectively. Notice that the scaling law of the curvaton-generated radiation is different from the usual radiation and it can be written as [40]

$$\rho_{r\sigma} \propto a^{-p}, \quad (103)$$

with $p = 3/2$ during the curvaton-dominated (matter-dominated) epoch and $p = 1$ during the radiation-dominated epoch. With the above parametrization, the equation of state for the curvaton-generated radiation can be written as $1 + w_{r\sigma} = p/3$ and its perturbation is given by

$$\zeta_{r\sigma} = \delta N + \frac{1}{p} \ln \left(\frac{\rho_{r\sigma}(t, \vec{x})}{\bar{\rho}_{r\sigma}(t)} \right). \quad (104)$$

From the above equation, one can write its energy density as

$$\rho_{r\sigma}(t, \vec{x}) = \bar{\rho}_{r\sigma}(t) e^{p(\zeta_{r\sigma} - \delta N)}. \quad (105)$$

As for the inflaton-generated radiation, its energy density scales as $\rho_{r\phi} \propto a^{-4}$, which implies $\rho_{r\phi}(t, \vec{x}) = \bar{\rho}_{r\phi}(t) e^{4(\zeta_{r\phi} - \delta N)}$.

Taking into account the two radiation components, the temperature is given by

$$T \equiv \left[\frac{30}{\pi^2 g_*} (\rho_{r\phi} + \rho_{r\sigma}) \right]^{1/4}, \quad (106)$$

and the temperature fluctuations are related to the radiation perturbations $\zeta_{r\phi}$ and $\zeta_{r\sigma}$ according to the expression

$$\delta_T = (1 - f)(\zeta_{r\phi} - \delta N) + \frac{p}{4} f(\zeta_{r\sigma} - \delta N), \quad (107)$$

where we have introduced the fraction of the curvaton-generated radiation in the total radiation component,

$$f \equiv \frac{\rho_{r\sigma}}{\rho_r} = \frac{\rho_{r\sigma}}{\rho_{r\phi} + \rho_{r\sigma}}. \quad (108)$$

Evaluating δ_T at the transition time and using Eqs. (17) and (107), we obtain

$$\delta N_{\mathcal{H}} = \frac{1}{3\tilde{\Omega} - 2\alpha(1 - f + fp/4)} \left(3 \sum_i \tilde{\Omega}_i \zeta_i - 2\alpha(1 - f)\zeta_{r\phi} - \frac{1}{2}\alpha fp \zeta_{r\sigma} \right). \quad (109)$$

When $f = 0$ (i.e., no curvaton-generated radiation), the above expression reduces to Eq. (22). Since we separate the radiation component into the curvaton- and inflaton-generated ones, $\tilde{\Omega}$ and $\sum_i \tilde{\Omega}_i \zeta_i$ are written as

$$3\tilde{\Omega} = 4\Omega_{r\phi} + 3\Omega_\sigma + p\Omega_{r\sigma}, \quad (110)$$

$$3\sum_i \tilde{\Omega}_i \zeta_i = 4\Omega_{r\phi}\zeta_{r\phi} + 3\Omega_\sigma\zeta_\sigma + p\Omega_{r\sigma}\zeta_{r\sigma}. \quad (111)$$

Furthermore, by equating $\rho_{r\sigma}$ and ρ_σ at the time of the curvaton decay as^{#8}

$$\bar{\rho}_{r\sigma} e^{p(\zeta_{r\sigma} - \delta N_{\text{dec}})} = \bar{\rho}_\sigma e^{3(\zeta_\sigma - \delta N_{\text{dec}})}, \quad (112)$$

at linear order, we can relate $\zeta_{r\sigma}$ and ζ_σ as follows:

$$p\zeta_{r\sigma} = [3 + (p-3)r_{\text{dec}}]\zeta_\sigma, \quad (113)$$

where we have used the fact that $\delta N_{\text{dec}} = r_{\text{dec}}\zeta_\sigma$ with r_{dec} being given by

$$r_{\text{dec}} = \left. \frac{3\Omega_\sigma + 3\Omega_{r\sigma}}{4\Omega_{r\phi} + 3\Omega_\sigma + 3\Omega_{r\sigma}} \right|_{\text{dec}}, \quad (114)$$

which is a generalization of the one given in Eq. (13).

We now consider the CDM perturbation ζ_c . From Eqs. (24) and (25), we can write

$$\zeta_c = \frac{1}{3}(\nu\delta_T + 3\delta N_{\mathcal{H}}). \quad (115)$$

In the simplest curvaton scenarios, the inflaton fluctuations are negligible compared to those of the curvaton and we thus set $\zeta_{r\phi} = 0$. Substituting the expressions for δ_T and $\delta N_{\mathcal{H}}$ given in Eqs. (107) and (109), we finally obtain

$$\zeta_c = \frac{1}{3} \left[\frac{\nu f}{4} (3 + (p-3)r_{\text{dec}}) + \left\{ 3 - \nu \left(1 - f + \frac{fp}{4} \right) \right\} \left(\frac{3\Omega_\sigma + (\Omega_{r\sigma} - \alpha f/2)(3 + (p-3)r_{\text{dec}})}{4 - \Omega_\sigma + (p-4)\Omega_{r\sigma} - 2\alpha(1 - f + fp/4)} \right) \right] \zeta_\sigma. \quad (116)$$

Notice that the above expression is a general formula where we just assumed $\Gamma = \Gamma(T)$, and all quantities on the right hand side, except r_{dec} , should be evaluated at the time of the transition. For the WIMP case, we can just set

$$\alpha = \frac{m}{T} + \frac{3}{2} + \frac{q}{2}, \quad \nu = \frac{m}{T} + \frac{3}{2}, \quad (117)$$

as already given in Eqs. (35) and (36). For the axion case, as given in Eq. (49), we can use

$$\alpha = \nu = -\beta. \quad (118)$$

^{#8} This relation can be considered to determine the normalization of the energy density of the curvaton-generated radiation.

From Eq. (116), we can easily see why the isocurvature fluctuations vanish even if CDM particles freeze out before the curvaton decay, or the axion begins to oscillate before the curvaton decay when the curvaton-generated radiation dominates in the radiation component. In such cases, the radiation energy density is $\rho_r \simeq \rho_{r\sigma}$, which corresponds to $f \simeq 1$ and $\Omega_{r\phi} \ll \Omega_{r\sigma}, \Omega_\sigma$. Therefore, by evaluating ζ_c using Eq. (116) with

$$f \simeq 1, \quad r_{\text{dec}} = 1, \quad \Omega_\sigma + \Omega_{r\sigma} \simeq 1, \quad (119)$$

we obtain $\zeta_c \simeq \zeta_\sigma$, which means that $S_c \simeq 0$. Hence the isocurvature perturbation is suppressed even if the transition, such as the WIMP freeze-out or the onset of axion oscillations of the axion, occurs before the curvaton decay, as confirmed by the numerical treatment discussed in the main text.

B Another analytic expression for Ω_{WIMP}

The goal of this appendix is to derive a more precise estimate of the final Ω_{WIMP} , inspired by Ref. [39].

Following Ref. [39], let us introduce a variable \mathcal{F} defined as

$$\mathcal{F} \equiv \frac{n_{\text{WIMP}} a^3}{a_{\text{fr}}^3 T_{\text{fr}}^3}, \quad (120)$$

where a subscript “fr” denotes a time of the WIMP freeze-out defined in the following (see Eq. (123)). It should be noticed that the definition of the freeze-time in this appendix is different from the one adopted in the main text.

By using this variable, the evolution equation for n_{WIMP} can be written as

$$\frac{d\mathcal{F}}{dt} + \lambda n_{\text{WIMP}} \mathcal{F} = \lambda \frac{a_{\text{fr}}^3 T_{\text{fr}}^3}{a^3} (\mathcal{F}^{(\text{eq})})^2. \quad (121)$$

In the above equation, we can identify two time scales, τ_{rel} and τ_{eq} , respectively defined by

$$\begin{aligned} \tau_{\text{rel}}^{-1} &= \lambda n_{\text{WIMP}}, \\ \tau_{\text{eq}}^{-1} &= -\frac{d}{dt} \ln [(\mathcal{F}^{(\text{eq})})^2 a^{-3}] = -3H - 2 \left(\frac{3}{2} + \frac{m_{\text{WIMP}}}{T} \right) \frac{d \ln T}{dt}, \end{aligned} \quad (122)$$

and the freeze-out corresponds to the instant when these two time scales coincide, i.e.

$$\tau_{\text{rel}}(t_{\text{fr}}) = \tau_{\text{eq}}(t_{\text{fr}}). \quad (123)$$

After freeze-out, the right hand side of Eq. (121) becomes negligible, the equation for \mathcal{F} reduces to

$$\frac{d\mathcal{F}}{dt} + \lambda \frac{a_{\text{fr}}^3 T_{\text{fr}}^3}{a^3} \mathcal{F}^2 \simeq 0. \quad (124)$$

This equation means that \mathcal{F} slightly evolves in time even after the freeze-out time, and by integrating this equation, we obtain

$$\mathcal{F}(t) = \frac{\mathcal{F}_{\text{fr}}}{1 + \mu(t)}, \quad (125)$$

where we have introduced an evolution factor $\mu(t)$, defined by

$$\mu(t) = \lambda n_{\text{WIMP},\text{fr}} \int_{t_{\text{fr}}}^t e^{-3(N-N_{\text{fr}})} dt. \quad (126)$$

Using the above expression, Ω_{WIMP} is given by

$$\begin{aligned} \Omega_{\text{WIMP}} h^2 &= \frac{m_{\text{WIMP}} n_{\text{WIMP},0}}{\rho_{\text{crit}}/h^2} = \frac{m_{\text{WIMP}}}{\rho_{\text{crit}}/h^2} \left(\frac{a_c}{a_0}\right)^3 n_{\text{WIMP},c} \\ &= m_{\text{WIMP}} \frac{s_0}{\rho_{\text{crit}}/h^2} \left(\frac{a_c^3 s_c}{a_0^3 s_0}\right) \frac{n_{\text{WIMP},c}}{s_c} \\ &\simeq 0.12 \left(\frac{m_{\text{WIMP}}/T_{\text{fr}}}{20}\right) \left(\frac{3.3 \times 10^9 \text{ GeV}^{-1}}{\lambda M_{\text{pl}}}\right) (1 - \Omega_{\sigma,\text{fr}})^{-1/2} \frac{1}{1 + \mu_0} \\ &\quad \times \left[-3 - 2 \left(\frac{3}{2} + \frac{m_{\text{WIMP}}}{T_{\text{fr}}}\right) \frac{d \ln T}{dN} \Big|_{t=t_{\text{fr}}} \right] \times \begin{cases} 1 & \text{for } T_c < T_{\text{dec}} \\ R_s^{-1} & \text{for } T_c > T_{\text{dec}} \end{cases}, \quad (127) \end{aligned}$$

where μ_0 is evaluated at $t = t_0$ and we have assumed $T_{\text{fr}} \simeq T_c$.

References

- [1] P. A. R. Ade *et al.* [Planck Collaboration], *Astron. Astrophys.* **594**, A13 (2016) [arXiv:1502.01589 [astro-ph.CO]].
- [2] P. A. R. Ade *et al.* [Planck Collaboration], *Astron. Astrophys.* **594**, A20 (2016) [arXiv:1502.02114 [astro-ph.CO]].
- [3] K. Enqvist and M. S. Sloth, *Nucl. Phys. B* **626**, 395 (2002) [hep-ph/0109214].
- [4] D. H. Lyth and D. Wands, *Phys. Lett. B* **524**, 5 (2002) [hep-ph/0110002].
- [5] T. Moroi and T. Takahashi, *Phys. Lett. B* **522**, 215 (2001) [Erratum-ibid. **B 539**, 303 (2002)] [hep-ph/0110096].
- [6] P. A. R. Ade *et al.* [BICEP2 and Keck Array Collaborations], *Phys. Rev. Lett.* **116**, 031302 (2016) [arXiv:1510.09217 [astro-ph.CO]].
- [7] T. Moroi and T. Takahashi, *Phys. Rev. D* **66**, 063501 (2002) [hep-ph/0206026].

- [8] D. H. Lyth, C. Ungarelli and D. Wands, Phys. Rev. D **67**, 023503 (2003) [astro-ph/0208055].
- [9] D. H. Lyth and D. Wands, Phys. Rev. D **68**, 103516 (2003) [astro-ph/0306500].
- [10] M. Lemoine and J. Martin, Phys. Rev. D **75**, 063504 (2007) [astro-ph/0611948].
- [11] T. Moroi and T. Takahashi, Phys. Lett. B **671**, 339 (2009) [arXiv:0810.0189 [hep-ph]].
- [12] T. Takahashi, M. Yamaguchi and S. Yokoyama, Phys. Rev. D **80**, 063524 (2009) [arXiv:0907.3052 [astro-ph.CO]].
- [13] A. A. Starobinsky, JETP Lett. **42**, 152 (1985) [Pisma Zh. Eksp. Teor. Fiz. **42**, 124 (1985)].
- [14] D. S. Salopek and J. R. Bond, Phys. Rev. D **42**, 3936 (1990).
- [15] M. Sasaki and E. D. Stewart, Prog. Theor. Phys. **95**, 71 (1996) [astro-ph/9507001].
- [16] M. Sasaki and T. Tanaka, Prog. Theor. Phys. **99**, 763 (1998) [gr-qc/9801017].
- [17] D. Langlois and A. Lepidi, JCAP **1101**, 008 (2011) [arXiv:1007.5498 [astro-ph.CO]].
- [18] D. Langlois and T. Takahashi, JCAP **1304**, 014 (2013) [arXiv:1301.3319 [astro-ph.CO]].
- [19] D. Langlois and F. Vernizzi, Phys. Rev. D **70**, 063522 (2004) [astro-ph/0403258].
- [20] T. Moroi, T. Takahashi and Y. Toyoda, Phys. Rev. D **72**, 023502 (2005) [arXiv:hep-ph/0501007].
- [21] T. Moroi and T. Takahashi, Phys. Rev. D **72**, 023505 (2005) [arXiv:astro-ph/0505339];
- [22] D. Langlois, F. Vernizzi and D. Wands, JCAP **0812**, 004 (2008) [arXiv:0809.4646 [astro-ph]].
- [23] K. Ichikawa, T. Suyama, T. Takahashi and M. Yamaguchi, Phys. Rev. D **78**, 023513 (2008) [arXiv:0802.4138 [astro-ph]].
- [24] K. Enqvist and T. Takahashi, JCAP **1310**, 034 (2013) [arXiv:1306.5958 [astro-ph.CO]].
- [25] N. Kitajima, D. Langlois, T. Takahashi, T. Takesako and S. Yokoyama, JCAP **1410**, 032 (2014) [arXiv:1407.5148 [astro-ph.CO]].
- [26] R. D. Peccei and H. R. Quinn, Phys. Rev. Lett. **38**, 1440 (1977).
- [27] R. D. Peccei and H. R. Quinn, Phys. Rev. D **16**, 1791 (1977).
- [28] S. Weinberg, Phys. Rev. Lett. **40**, 223 (1978).

- [29] F. Wilczek, Phys. Rev. Lett. **40**, 279 (1978).
- [30] M. Kawasaki and K. Nakayama, Ann. Rev. Nucl. Part. Sci. **63**, 69 (2013) [arXiv:1301.1123 [hep-ph]].
- [31] D. J. E. Marsh, Phys. Rept. **643**, 1 (2016) [arXiv:1510.07633 [astro-ph.CO]].
- [32] O. Wantz and E. P. S. Shellard, Phys. Rev. D **82**, 123508 (2010) [arXiv:0910.1066 [astro-ph.CO]].
- [33] D. Langlois, Phys. Rev. D **59**, 123512 (1999) [astro-ph/9906080].
- [34] D. Langlois and T. Takahashi, JCAP **1102**, 020 (2011) [arXiv:1012.4885 [astro-ph.CO]].
- [35] D. Langlois and B. van Tent, Class. Quant. Grav. **28**, 222001 (2011) [arXiv:1104.2567 [astro-ph.CO]].
- [36] D. Langlois and B. van Tent, JCAP **1207**, 040 (2012) [arXiv:1204.5042 [astro-ph.CO]].
- [37] C. Hikage, M. Kawasaki, T. Sekiguchi and T. Takahashi, JCAP **1303**, 020 (2013) [arXiv:1212.6001 [astro-ph.CO]].
- [38] P. A. R. Ade *et al.* [Planck Collaboration], Astron. Astrophys. **594**, A17 (2016) [arXiv:1502.01592 [astro-ph.CO]].
- [39] P. Salati, Phys. Lett. B **571**, 121 (2003) [astro-ph/0207396].
- [40] E. Kolb and M. Turner, *The Early Universe*, Westview Press (1994)
- [41] L. J. Hall, K. Jedamzik, J. March-Russell and S. M. West, JHEP **1003**, 080 (2010) [arXiv:0911.1120 [hep-ph]].
- [42] Y. Hochberg, E. Kuflik, T. Volansky and J. G. Wacker, Phys. Rev. Lett. **113**, 171301 (2014) [arXiv:1402.5143 [hep-ph]].
- [43] Y. Hochberg, E. Kuflik, H. Murayama, T. Volansky and J. G. Wacker, Phys. Rev. Lett. **115**, no. 2, 021301 (2015) [arXiv:1411.3727 [hep-ph]].